



The electrostatic nature of contaminative particles in a semiconductor processing plasma

Item Type	text; Thesis-Reproduction (electronic)
Authors	Nowlin, Robert Nathaniel, 1966-
Publisher	The University of Arizona.
Rights	Copyright © is held by the author. Digital access to this material is made possible by the University Libraries, University of Arizona. Further transmission, reproduction or presentation (such as public display or performance) of protected items is prohibited except with permission of the author.
Download date	23/08/2022 08:04:49
Link to Item	http://hdl.handle.net/10150/277802

INFORMATION TO USERS

The most advanced technology has been used to photograph and reproduce this manuscript from the microfilm master. UMI films the text directly from the original or copy submitted. Thus, some thesis and dissertation copies are in typewriter face, while others may be from any type of computer printer.

The quality of this reproduction is dependent upon the quality of the copy submitted. Broken or indistinct print, colored or poor quality illustrations and photographs, print bleedthrough, substandard margins, and improper alignment can adversely affect reproduction.

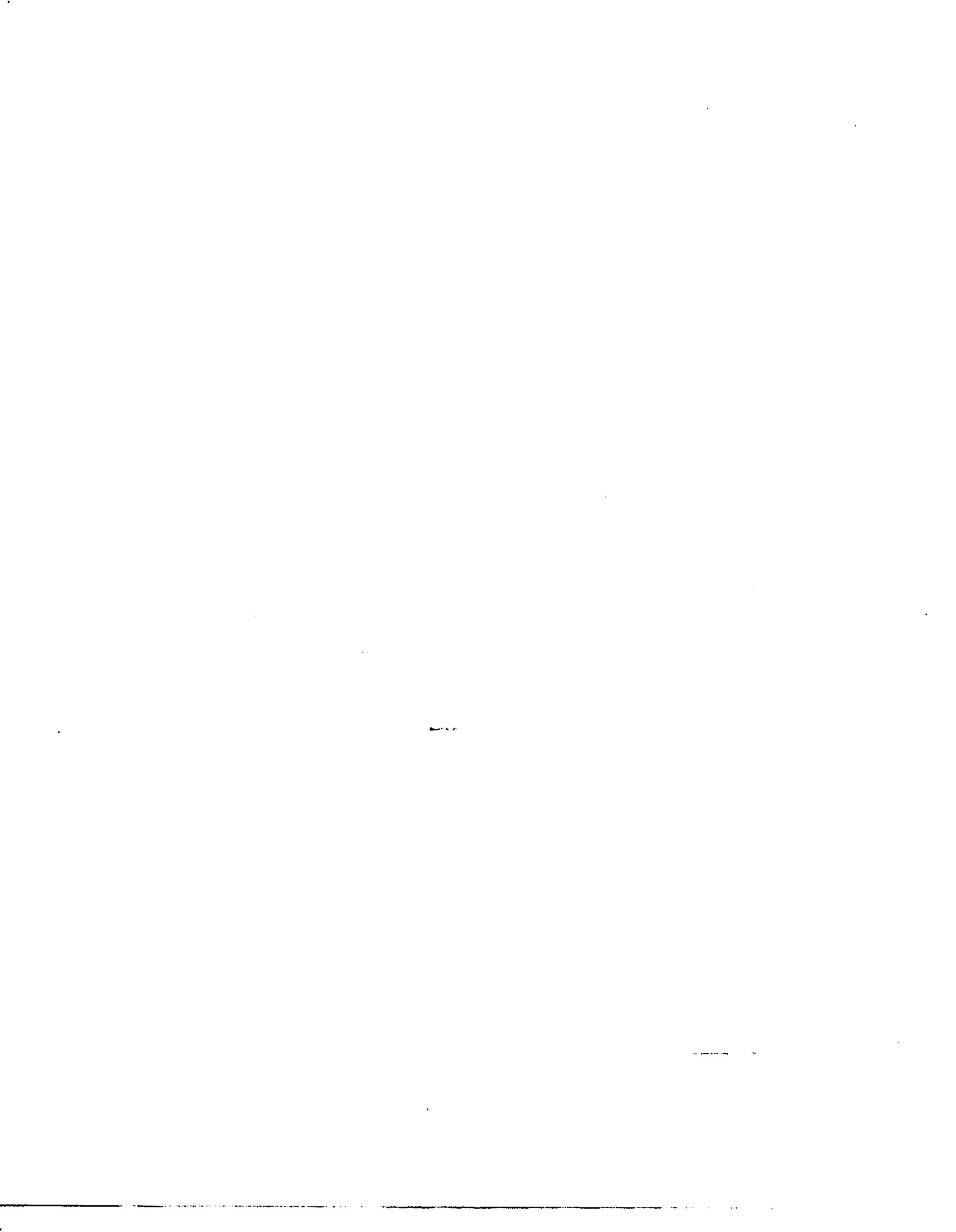
In the unlikely event that the author did not send UMI a complete manuscript and there are missing pages, these will be noted. Also, if unauthorized copyright material had to be removed, a note will indicate the deletion.

Oversize materials (e.g., maps, drawings, charts) are reproduced by sectioning the original, beginning at the upper left-hand corner and continuing from left to right in equal sections with small overlaps. Each original is also photographed in one exposure and is included in reduced form at the back of the book.

Photographs included in the original manuscript have been reproduced xerographically in this copy. Higher quality 6" x 9" black and white photographic prints are available for any photographs or illustrations appearing in this copy for an additional charge. Contact UMI directly to order.

U·M·I

University Microfilms International
A Bell & Howell Information Company
300 North Zeeb Road, Ann Arbor, MI 48106-1346 USA
313/761-4700 800/521-0600



Order Number 1342981

**The electrostatic nature of contaminative particles in a
semiconductor processing plasma**

Nowlin, Robert Nathaniel, M.S.

The University of Arizona, 1990

U·M·I
300 N. Zeeb Rd.
Ann Arbor, MI 48106



**THE ELECTROSTATIC NATURE OF
CONTAMINATIVE PARTICLES IN A
SEMICONDUCTOR PROCESSING PLASMA**

by

Robert Nathaniel Nowlin


A Thesis Submitted to the Faculty of the
DEPARTMENT OF ELECTRICAL AND COMPUTER ENGINEERING
In Partial Fulfillment of the Requirements
For the Degree of
MASTER OF SCIENCE
WITH A MAJOR IN ELECTRICAL ENGINEERING
In the Graduate College
THE UNIVERSITY OF ARIZONA

1990

STATEMENT BY AUTHOR

This thesis has been submitted in partial fulfillment of requirements for an advanced degree at The University of Arizona and is deposited in the University Library to be made available to borrowers under rules of the library.

Brief quotations from this thesis are allowable without special permission, provided that accurate acknowledgment of source is made. Requests for permission for extended quotation from or reproduction of this manuscript in whole or in part may be granted by the head of the major department or the Dean of the Graduate College when in his or her judgment the proposed use of the material is in the interests of scholarship. In all other instances, however, permission must be obtained from the author.

SIGNED: 

APPROVAL BY THESIS DIRECTOR

This thesis has been approved on the date shown below:



R. N. Carlile

Professor of Electrical and Computer Engineering

11/6/90

Date

ACKNOWLEDGMENTS

I would like to extend my deepest gratitude to Dr. Robert N. Carlile. From the inception of this project to its completion, he has been an indispensable mentor and guide. His encouragement and enduring confidence served as a continual motivation. I am indebted to him for his many contributions to this work.

I also want to thank my dear wife, Sandy, who, for the first seven months of our marriage, lovingly endured the many hours this work stole from her.

TABLE OF CONTENTS

	page
LIST OF FIGURES	7
ABSTRACT	9
CHAPTER 1 – INTRODUCTION	10
1.1 PURPOSE OF WORK	10
1.2 REVIEW OF CURRENT WORK	10
1.3 PREVIEW OF THESIS	12
CHAPTER 2 – POISSON MODEL	14
2.1 THEORY	14
2.1.1 Definitions	14
2.1.2 Dynamics	15
2.1.3 Conservation of Energy	18
2.1.4 Negative Charge Number Density	19
2.1.5 Positive Charge Number Density	21
2.1.6 Flux Densities	23
2.1.7 Poisson’s Equation	26
2.2 NUMERICAL TECHNIQUES	26
2.2.1 Normalized Equations	26
2.2.2 Boundary Conditions and Constraints	27
2.2.3 Strategy of Integration	29
2.2.4 Conversion to Physical Parameters	33
2.3 RESULTS	33
2.3.1 Critical Contaminant Radius	33

	5
2.3.2 Choosing x_0	34
2.3.3 Voltage Characteristics	39
2.3.4 Flux Characteristics	42
2.3.5 Electric Field Characteristics	42
2.3.6 Charge Characteristics	44
2.4 SUMMARY	47
CHAPTER 3 – COULOMB MODEL	48
3.1 THEORY	48
3.1.1 Justification	48
3.1.2 Central Force Equations	48
3.1.3 Conservation of Energy	53
3.1.4 Positive Charges	54
3.1.5 Negative Charges	56
3.2 RESULTS	58
3.2.1 Voltage Characteristics	58
3.2.2 Flux Characteristics	59
3.2.3 Charge Characteristics	61
3.2.4 Electric Field Characteristics	62
3.3 SUMMARY	63
CHAPTER 4 – CONCLUSION	64
4.1 POISSON MODEL SUMMARY	64
4.2 COULOMB MODEL SUMMARY	64
4.3 COMPARISON OF THE TWO MODELS	65
4.4 SUGGESTIONS FOR CONTINUED STUDY	66
APPENDIX A – PROGRAM LISTING FOR COMPUTATIONS WITH THE POISSON MODEL	68

REFERENCES 95

LIST OF FIGURES

	page
Fig. 2.1 Particle with Sheath	16
Fig. 2.2 Velocity Components	18
Fig. 2.3 Limits of Integration for Negative Charges	20
Fig. 2.4 Effective Potential Energy for Positive Charges	22
Fig. 2.5 Limits of Integration for Positive Charges	24
Fig. 2.6 Plots of Eq. (2.31), λ vs. x_0	30
Fig. 2.7 Plots of Eq. (2.32), y_a vs. x_a	32
Fig. 2.8 Typical Normalized Solution Showing Conditions for the Critical Contaminant Radius	35
Fig. 2.9a Critical Contaminant Radius Characteristics	35
Fig. 2.9b Debye Length, for Comparison to Fig. 2.9a	35
Fig. 2.10 The Relationship Between x_0 and a	36-38
Fig. 2.11 Typical Normalized Solutions, General Cases	40
Fig. 2.12 Typical Physical Solutions for the Same Cases as in Fig. 2.11	40
Fig. 2.13 Contaminant Voltage Characteristics	41
Fig. 2.14 Particulate Flux to the Contaminant Surface	43
Fig. 2.15 Electric Field Distributions for the Same Cases as in Fig. 2.11	44
Fig. 2.16 Surface Electric Field Characteristics	45
Fig. 2.17 Contaminant Charge Characteristics	46
Fig. 3.1 The Geometry of a Typical Particulate Trajectory	50
Fig. 3.2 Vector Rotation as a Particle Moves Along its Trajectory	51

Fig. 3.3 The Geometry of a Hyperbolic Trajectory	55
Fig. 3.4 Normalized Contaminant Voltage	60
Fig. 3.5 Particulate Flux to the Contaminant Surface	61
Fig. 3.6 Contaminant Charge Characteristics	62
Fig. 3.7 Surface Electric Field Characteristics	62

ABSTRACT

Two models are presented to describe the immediate environment surrounding negatively charged contaminants in an idealized plasma. The first model uses Poisson's equation to determine the contaminant charge and voltage. This model predicts a critical radius of 40 microns or less below which Poisson's equation is no longer valid. For contaminant radii less than 40 microns, the Coulomb potential is used to find the contaminant charge and voltage. Both models predict negative charges on the order of 10^{-14} Coulombs, and voltages on the same order of magnitude as the electron energy.

CHAPTER 1

INTRODUCTION

1.1 PURPOSE OF WORK

Contaminative particles in semiconductor processing is a critical issue in the success of VLSI manufacturing. It is important to understand the origins of these contaminants and what effects they have on the process. Plasma etching is typically a very dirty process and leads to the generation of many contaminative particles. These contaminants can become negatively charged and be trapped in the plasma. If large numbers of these contaminants congregate in the plasma, they can adversely affect the plasma and change the resulting etches. Furthermore, these contaminants will fall on the wafer after the plasma is extinguished. In order to understand the behavior of these contaminants in the plasma and how they affect other properties of the plasma, it is necessary to understand their electrostatic behavior. This paper will present a theory describing this behavior and some numerical results regarding the characteristics of these contaminants. Two models will be developed describing contaminants of different sizes. These models can be used in plasma simulation codes to study the effects of the contaminants on the plasma.

1.2 REVIEW OF CURRENT WORK

Very little work has been done to date on the precise electrostatic nature of contaminants in a semiconductor processing plasma. One model proposed by Michael McCaughey and Mark Kushner approximates the potential distribution in the vicinity of a contaminant by the usual Debye shielded Coulomb potential that is used to describe a variety of plasma phenomena [1]. In particular, they propose a potential distribution

$$V(r) = V_a \frac{a}{r} e^{-(r-a)/\lambda_d}, \quad (1.1)$$

where a is the particle radius, V_a is the voltage at the particle, and λ_d is the Debye length. It is interesting to note that McCaughy and Kushner suggest that the particle will develop a negative charge if it is at least as large as the Debye length. Using the potential distribution (Eq. (1.1)) to determine the forces on the particle in the plasma, they conclude by means of a Monte Carlo simulation that the presence of particles in the plasma will shift the energy distribution of the electrons to lower energy.

Further theoretical work done at the University of California, Berkeley, uses a modified Debye potential [2]. In fact, in this work several different "shape transformations" are applied to Eq. (1.1). The result is that for contaminants with radii less than the Debye length, the actual shape of the potential is insignificant. It is further suggested that it may be necessary to include the effects of a cut-off Maxwellian distribution, and that this may lead to a reduced voltage on the contaminant.

Experimental evidence of the presence of contaminants in the plasma has been given by G. Selwyn, J. Singh, and R. Bennett [3]. Selwyn and coworkers used laser light scattering techniques to observe particles congregating near the sheath regions of the plasma. The fact that the contaminants are trapped in the plasma is evidence that they are negatively charged. This is further supported by the fact that they tend to collect at the sheath regions where there is a potential well for negatively charged particles. Furthermore, Selwyn and coworkers have noted that in the sheath region, the intensity of the glow discharge seems diminished. This seems to suggest a diminished electron temperature in agreement with McCaughy and Kushner. Selwyn, Singh, and Bennet have also collected these contaminants on silicon wafers and have analyzed them under a scanning electron microscope. They have noted that the contaminants are very nearly spherical, and that they have a crystalline structure, perhaps suggesting the presence of silicon in the particle. Selwyn and coworkers have reported that these contaminants have an average diameter of $23 \mu\text{m}$, comparable to the Debye length.

Other experimental work has been done by Selwyn, McKillop, Haller, and Wu [4], and Selwyn, Heidenreich, and Haller [5]. In [4], Selwyn, *et. al.*, conclude that mechanical stresses in a plasma system are responsible for the largest fluxes of contaminants, whereas the actual plasma process is responsible for the largest numbers of contaminants. The mechanical stresses are of very short duration in comparison to the time involved in the plasma process. Therefore, even though the plasma may produce contaminants at slower rates, more contaminants are produced due to the length of time involved. In [5], Selwyn, *et. al.*, have observed contaminant trapping regions that are dependent on the topography of the electrode. These trapping regions arise where there are spatial non-uniformities of the electrostatic fields near the sheath regions. It appears that the contaminants are trapped in potential wells that confine them in both the lateral and vertical directions. Selwyn, *et. al.*, [5] were also able to determine a lower bound on the number density of such trapped contaminants. Their estimate was a significantly large 10^7 contaminants per cm^{-3} .

1.3 PREVIEW OF THESIS

In view of such a large number of contaminants which may be present in a plasma, and the significant effects they may have on the plasma, the task of modeling the electrostatic environment of these contaminants becomes necessary. There are two models presented in this work. The first model is presented in chapter 2. This model is called the Poisson Model because it requires integration of Poisson's equation to determine the contaminant voltage and charge. The development followed in chapter 2 follows those of Swift and Schwar [6] and Bernstein and Rabinowitz [7]. These authors developed expressions for number densities, particulate fluxes, and Poisson's equation for spherical Langmuir probes. In chapter 2, similar expressions are developed for spherical contaminants. Boundary conditions for the problem are developed, and a strategy of applying these boundary conditions is discussed. Results of the calculations with this model are also included in chapter 2.

The Poisson model developed in chapter 2 predicts a critical radius below which Poisson's equations break down. This radius is quite large, being about the same order of magnitude as the Debye length. Therefore, in chapter 3, a model for contaminants with radii smaller than the critical radius is developed. Since Poisson's equations are not valid for contaminants this small, a Coulomb central force is used to describe the trajectory of charged particles around the contaminant. This model is called the Coulomb Model. As in chapter 2, expressions for the particulate flux to the contaminant are developed. These equations lead to a direct determination of contaminant charge and voltage. Results of calculations with the Coulomb model are presented in chapter 3. Finally, chapter 4 will present a summary and comparison of the two models.

CHAPTER 2

POISSON MODEL

2.1 THEORY

In this chapter, a model of the electrostatic environment near a contaminative particle will be developed. This model is based upon integration of Poisson's equation which includes the effects of charged particles in the vicinity of a contaminant. The plasma under consideration will first be defined. A discussion of the mechanisms by which the contaminant becomes charged will follow. Based upon the qualitative understanding of the particle dynamics, considering the conservation of energy will lead to expressions for the number density and flux density of both positive and negative charges. These expressions can then be incorporated into Poisson's equation. Following the development of the differential equation, the solution techniques employed will be discussed. There are several normalized variables that prove useful in understanding the model. These variables and their importance will be explained. Next, the boundary conditions to the problem will be defined, followed by a discussion of the method of integration. Finally, the results of these calculations will be presented and interpreted.

2.1.1 Definitions

In this work, a plasma will be defined as a gaseous collection of four species of particles. The primary constituent of the plasma is the neutral species of atoms. These particles are uncharged and very massive, and they do not contribute to the electrostatics of the contaminants. A semiconductor processing plasma is typically a weakly ionized gas, and therefore only a small percentage of the particles are charged. Some of these particles are very massive positive ions. They are very sluggish in their motion, and for reasons of mathematical simplicity, the energy distribution of the positive ions is assumed to be a delta function at an energy

E_0 . The remaining particles are negatively charged. These particles are the massive negative ions and the highly mobile electrons. It is assumed that the energy distribution of both of these species is Maxwellian. The net numbers of positive and negative charges in the bulk of the plasma (at a distance $r = \infty$ from the contaminant) exactly balance to maintain charge conservation:

$$N_+(\infty) = N_e(\infty) + N_-(\infty). \quad (2.1)$$

Here N_+ is the number density of positive ions, N_e is the number density of electrons, and N_- is the number density of negative ions. In writing Eq. (2.1), it is assumed that the plasma as a whole is neutral. In the remainder of this paper, subscripts will be used to indicate the type of charge a specific variable relates to. In particular, positive charges will be denoted by a "+", negative ions by a "-", and electrons by an "e". Furthermore, the term "contaminant" will be used exclusively to refer to the large contaminative particle, whereas the term "particle" will refer to all the smaller, atomic particles that constitute the plasma, such as electrons and ions.

2.1.2 Dynamics

It is critical to note that the electrons are very mobile in the plasma, because it is their rapid motion that leads to the development of a negative charge on any surface in contact with the plasma. In particular, a contaminative particle immersed in a plasma will initially experience a rush of electrons to its surface. It is assumed that the surface is perfectly absorbing; secondary emission of electrons is neglected. Therefore, a repelling Coulomb force begins to reduce the flux of negative charges to the surface of the contaminant. This Coulomb force which repels negative charges will attract positive charges, thus forming a sheath region in which the number of positive charges exceeds the total number of negative charges (Fig. 2.1). This sheath region tends to shield the negatively charged contaminant in a manner similar to the Debye-screened potential (Eq. (1.1)). As will be seen, the true shielding is more complicated than this. However, higher energy electrons (and

occasionally some negative ions) will continue to overcome the repulsion and collide with the contaminant until the repulsion is so great that only negative charges with the highest energies can surmount the potential barrier. This will happen with a small frequency exactly equal to that of the arrival rate of an attracted positive charge.

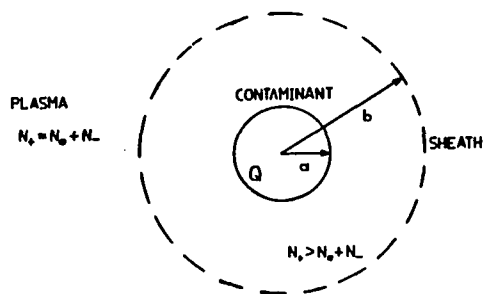


Fig. 2.1 A large contaminant immersed in a plasma will develop a sheath around it. In the sheath, the number density of positive charges is larger than the number density of negative charges. This is due to the negative charge, Q , on the contaminant. In comparison, in the bulk of the plasma, there is charge neutrality.

Therefore, the contaminant will develop some stable negative charge that will regulate the fluxes of positive and negative charges to its surface such that they are equal. In other words, the occasional ion that gets accelerated to the surface is quickly neutralized by an electron with energy high enough to overcome the potential. Expressing this mathematically, under equilibrium conditions, the fluxes of charges to the surface of the contaminant ($r = a$) satisfy

$$\Gamma_+(a) = \Gamma_-(a) + \Gamma_e(a) \quad (2.2)$$

where Γ represents the flux of each of the various charges denoted by the subscripts.

These same dynamics can be applied to any surface in the vicinity of the plasma. In particular, the walls of the containing chamber will also develop a

surface layer of electrons. Therefore, an electric field develops between the plasma and all other surfaces that points from the plasma to the surface. This electric field then repels negative charges back into the plasma. Therefore, contaminants in the plasma will be trapped there until the plasma is extinguished.

On a more quantitative level, the contaminant will develop a negative charge Q that will in turn set up a potential V between the surface of the contaminant and the rest of the plasma. Normally, the presence of the charge Q will lead to the development of the Coulomb force, but in this case there are many other charges in the vicinity which will alter that force and shield other particles from it. Therefore, it is necessary to include the effects of the charge density distribution. The primary tool for this is Poisson's equation, namely:

$$\nabla^2 V(r) = -\frac{\rho(r)}{\epsilon_0}, \quad (2.3)$$

where ρ is the net charge density distribution, and ϵ_0 is the free space permittivity. Assuming the contaminants have a spherical geometry, and that there are no variations in the plasma in either of the angular directions (θ and ϕ), it is convenient to write Poisson's equation in spherical coordinates,

$$\frac{1}{r^2} \frac{d}{dr} \left(r^2 \frac{dV(r)}{dr} \right) = -\frac{e}{\epsilon_0} (N_+(r) - N_e(r) - N_-(r)), \quad (2.4)$$

where e is the elementary electronic charge. This can now be integrated directly to find the potential at the surface of the contaminant, and the charge that supports that potential.

The number density of each species of particles can be found by integrating the velocity distribution function over all of velocity space,

$$N(r) = \int \int \int f(u, w) w d\alpha dw du. \quad (2.5)$$

The velocity component in the radial direction is denoted by u , and in the angular or polar direction (θ), it is denoted by w as shown in Fig. 2.2. The quantity α (Fig. 2.2) is the azimuthal angle in velocity space. The distribution function is

given by $f(u, w)$. It is convenient to perform the integration in energy space, and by considering the conservation of energy, the velocities can be found in terms of total energy, E , and angular momentum, J . The expressions for the number density distributions of each species of charged particle will be developed below. For a more detailed discussion see Swift and Schwar [6] or Bernstein and Rabinowitz [7]. Bernstein and Rabinowitz originally developed the approach summarized in this chapter, but Swift and Schwar provide a very readable and understandable treatment of the same methods.

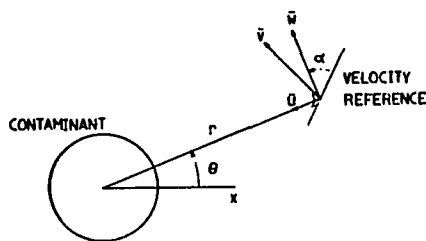


Fig. 2.2 Any arbitrary particulate velocity, v , can be decomposed into a radial component, u , and an angular component, w . The angular velocity, w , makes an angle, α , with some arbitrary reference velocity.

2.1.3 Conservation of Energy

The total energy is the sum of the kinetic energy and the potential energy,

$$E = \frac{m}{2}(u^2 + w^2) + qV, \quad (2.6)$$

where m is the mass of the charged particle, and q is its charge. The angular momentum is given by

$$J = mwr. \quad (2.7)$$

Therefore,

$$w = \frac{J}{mr}. \quad (2.8)$$

The total energy can then be expressed using the angular momentum as follows:

$$\begin{aligned} E &= \frac{mu^2}{2} + \left(\frac{J^2}{2mr^2} + qV \right) \\ &= \frac{mu^2}{2} + U, \end{aligned} \quad (2.9)$$

where

$$U = \left(\frac{J^2}{2mr^2} + qV \right) \quad (2.10)$$

is an effective potential energy. From Eq. (2.9) it is clear that

$$u = \sqrt{\frac{2(E - U)}{m}}. \quad (2.11)$$

With the substitution of equations (2.8) and (2.11) into Eq. (2.5), and after integrating in α from 0 to 2π , the integration becomes

$$N(r) = \frac{\pi}{m^2 r^2} \int_E \int_{J^2} \frac{f(E, J^2) dJ^2 dE}{\sqrt{2m(E - U)}}. \quad (2.12)$$

Now it only remains to determine the limits of integration for the energy and angular momentum of the various charged particles.

2.1.4 Negative Charge Number Density

For negative charges, the quantity U is always positive since the charge is negative and the potential is negative; that is, $qV > 0$. Therefore, for negative charges to have a positive radial kinetic energy, $\frac{1}{2}mu^2$, at a given radius, r , the total energy must exceed the effective potential energy ($E > U$) for any value of angular momentum. This can be expressed as

$$E > \frac{J^2}{mr^2} + qV(r).$$

Figure 2.3 shows a plot of the right hand side of the above inequality as a function of the square of angular momentum. Two curves are plotted; one for an arbitrary radius r , and one for a radius equal to the contaminant radius a . At a given radius, r , no particles exist with E - J^2 combinations in region A , because region

A corresponds to negative kinetic energies. Particles with $E-J^2$ combinations in region B will not have sufficient kinetic energy to overcome the repulsion and reach the radius a . Therefore, these particles will be reflected before reaching the contaminant, and will be counted twice in the integration for number density. Particles with $E-J^2$ values in region C will make it to the contaminant and be absorbed.

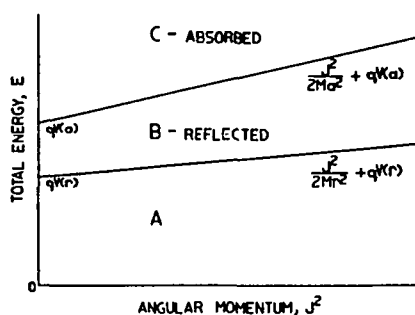


Fig. 2.3 A plot of the limits of integration for negative charge number density ($qV > 0$). Particles with energy and angular momentum in region A have negative radial kinetic energy, and hence they do not exist. Particles with energy and angular momentum in region B will penetrate to some radius less than a and be reflected. Particles with energy and angular momentum in region C will be absorbed by the probe. (After Bernstein and Rabinowitz [7].)

Therefore, integrating Eq. (2.12) over the regions indicated in Fig. 2.3, and assuming a Maxwellian energy distribution, the number density of negative charges in the vicinity of the contaminant is given as follows:

$$N(r) = N(\infty)e^{-qV(r)/kT}. \quad (2.13)$$

In arriving at this expression, it is further assumed that $V(r) \ll V(a)$ and $r \gg a$. The details of the integration are found in Swift and Schwar [6]. Here k is Boltzman's constant, T is the temperature of the species in question, and $N(\infty)$ is the number density in the bulk plasma (far from the contaminant). This equation

is applicable to both the electrons and the negative ions. Close to the contaminant, where V is largest, the number density of negative charges decays exponentially, that is, there are very few negative charges in the sheath region as expected.

2.1.5 Positive Charge Number Density

The situation is considerably more complex for positive charges. Since $q > 0$, the product of charge with voltage is negative: $qV < 0$. Therefore, the effective potential energy, U (Eq. (2.10)), can be either positive or negative depending on the relative magnitudes of J^2 , r^2 , and V . To show the behavior of U with radius, it is assumed that at large r , the potential V goes as $\frac{1}{r^2}$, and that at small r , the angular momentum term dominates. The resulting behavior of the effective potential energy is shown in Fig. 2.4. For $J^2 = 0$, U simply behaves as $qV(r)$. As J^2 increases, a minimum develops in the effective potential energy curves. This creates a potential well in which positive charges can become trapped. In this analysis it will be assumed that the populations of these traps will be sufficiently small to be neglected.

Furthermore, as J^2 increases still further, a maximum develops in the effective potential energy curve. Therefore, charges must have a kinetic energy sufficient to overcome this potential barrier in order to reach the contaminant. The character of the charge distribution changes at a critical point r_0 . This is the point where there is a maximum in the effective potential energy whose height is equal to the mono-energetic energy of the positive ions, E_0 . The value of angular momentum corresponding to this particular curve is J_0 . Positive ions with $J \geq J_0$ will never be attracted to the contaminant but will have a turning point at some radius r_0 or greater. Positive ions with $J < J_0$ will be attracted toward the contaminant and will be absorbed if the effective potential energy curve for that particle intersects the radius of the contaminant. Otherwise, the positive ion will have a turning

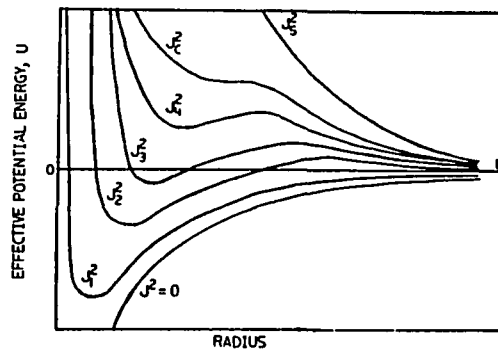


Fig. 2.4 A plot of the effective potential energy curves for positive charges for various values of angular momentum. As angular momentum increases from the bottom to the top, the curves develop minima and maxima until a critical value is reached where the curve has only an inflection point. Beyond this value of angular momentum, the curves are monotonically decreasing. (After Bernstein and Rabinowitz [7].)

point at some radius between a and r_0 . This change of character of the charge distribution can also be seen by understanding that the charge distribution is arrived at by integrating the energy distribution. Since the energy distribution is taken to be a delta function at E_0 , the integration defined in Eq. (2.5) produces a step function at r_0 .

As in the case of negative charges, there will be three regions defined in the E - J^2 space. There will be certain combinations of energy and angular momentum which will be excluded for positive charges at a particular radius. Region A in Fig. 2.5 corresponds to combinations of energy and angular momentum that are excluded on the basis of negative kinetic energy. The charges that will be attracted to the contaminant have E - J^2 values in region B . Region C represents those charges that will be reflected at some intermediate radius. These regions define the limits of the integration (2.5). The result of this integration yields the following

expression for the number density of positive charges:

$$N_+(r) = \frac{N_+(\infty)}{2} \left[\left(1 - \frac{eV(r)}{E_0} \right)^{\frac{1}{2}} \pm \left(1 - \frac{eV(r)}{E_0} - \frac{I_+}{I_r} \right)^{\frac{1}{2}} \right]. \quad (2.14)$$

The plus sign is used when $r \geq r_0$, and the negative sign is used when $r \leq r_0$. The radius r_0 is defined by

$$1 - \frac{eV(r_0)}{E_0} - \frac{I_+}{I_{r_0}} = 0 \quad (2.15a)$$

$$\frac{d}{dr} \left(1 - \frac{eV(r)}{E_0} - \frac{I_+}{I_r} \right)_{r=r_0} = 0. \quad (2.15b)$$

Furthermore,

$$I_r = \pi r^2 e N_+(\infty) \sqrt{\frac{2E_0}{M_+}} \quad (2.16)$$

where M_+ is the atomic mass of the positive charges. The term I_+ is the current of positive charges to the surface of the contaminant. This current is determined from the flux density as discussed in the next section.

2.1.6 Flux Densities

The current I_+ is given by

$$I_+ = 4\pi a^2 e \Gamma(a)$$

where $\Gamma(a)$ is given by the flux

$$\Gamma(r) = \int \int \int f(u, w) u w d\alpha dw du$$

evaluated at $r = a$. Substituting equations (2.8) and (2.11) into this expression yields

$$\Gamma(r) = \frac{1}{m^3 r^2} \int_{\alpha} \int_{J^2} \int_E f(E, J^2) d\alpha dJ^2 dE. \quad (2.17)$$

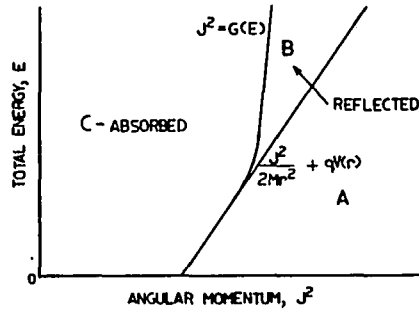


Fig. 2.5 A plot of the limits of integration for positive charge number density ($qV < 0$). Particles with energy and angular momentum in region A have negative radial kinetic energy, and hence they do not exist. Particles with energy and angular momentum in region B will penetrate to some radius less than a and be reflected. Particles with energy and angular momentum in region C will be absorbed by the probe. The curve, $G(E)$, is determined from the minima and maxima in Fig. 2.4. (After Bernstein and Rabinowitz [7].)

The form of the integrand for positive charges is very complicated. The problem is greatly simplified by the use of Eq. (2.2). The positive charge current can be found as the sum of the negative ion current and the electron current.

Performing the integration for negative charges can be easily done with the substitution of the Maxwellian distribution function into Eq. (2.17). The Maxwellian distribution function is given by

$$f_M(E) = \frac{N}{\pi^{\frac{3}{2}} v_t^3} e^{-E/kT},$$

where v_t is the thermal velocity,

$$v_t = \sqrt{\frac{2kT}{m}}.$$

Therefore, the flux of negative charges to the contaminant can be calculated as follows:

$$\Gamma(r) = \frac{N}{\pi^{\frac{1}{2}} v_t^3 m^3 r^2} \int_E \int_{J^2} e^{-E/kT} dJ^2 dE. \quad (2.18)$$

The integration in α has been performed from 0 to 2π . It is only necessary to determine the limits of integration for Eq. (2.18). Particles with total energy larger than the potential energy necessary to overcome the repulsive force of the contaminant will collide with the contaminant. That is, $E \geq qV$, where qV is now positive ($q = -e$). Furthermore, the limits on J^2 are determined by requiring the radial kinetic energy to be positive. This can be expressed as

$$J^2 \leq 2mr^2(E - qV).$$

For the particle to collide with the contaminant, this condition must be met at $r = a$. Therefore, inserting these limits into Eq. (2.18), the result is

$$\Gamma(r) = \frac{N}{\pi^{\frac{1}{2}} v_i^3 m^3 r^2} \int_{qV}^{\infty} \int_0^{2mr^2(E-qV)} e^{-E/kT} dJ^2 dE.$$

Finally, the flux of negatively charged particles to the contaminant is found by carrying out this simple integration, namely

$$\Gamma(a) = \frac{N}{4} \sqrt{\frac{8kT}{\pi m}} e^{-qV_a/kT}. \quad (2.19)$$

The voltage at the surface of the contaminant ($r = a$) is denoted by V_a .

Therefore, Eq. (2.19) gives the flux of a particular species of negative charge arriving at the surface of the contaminant. The quantity Γ represents a flux of particles per unit area. To obtain the current, Γ must be multiplied by the electronic charge, the valence of the ion, and by the surface area of the contaminant. In this work, only monovalent ions are considered. Therefore, the positive ion current can be given by the sum of the two negative-charge current components, (Eq. (2.2)):

$$I_+ = \pi a^2 e \left[N_e(\infty) \sqrt{\frac{8kT_e}{\pi m_e}} e^{eV_a/kT_e} + N_- \sqrt{\frac{8kT_-}{\pi M_-}} e^{eV_a/kT_-} \right], \quad (2.20)$$

where the quantity $q = -e$ has been substituted. The first term in the above equation represents the flux of electrons to the surface of the contaminant, and

the second term represents the flux of negative ions to the surface of the contaminant. Note that the reciprocal of the negative ion energy, kT_-/e , appears in the exponential of the negative ion flux term. This energy is very small, and since the voltage is negative, the negative ion flux term will be negligibly small.

2.1.7 Poisson's Equation

Expressions for the number density distributions of each species of charged particle in Poisson's equation have now been developed. Substituting these expressions into Eq. (2.4) yields the following form of Poisson's equation:

$$\frac{1}{r^2} \frac{d}{dr} \left(r^2 \frac{dV(r)}{dr} \right) = -\frac{eN_+(\infty)}{\epsilon_0} \left[\frac{1}{2} \left(1 - \frac{eV(r)}{E_0} \right)^{\frac{1}{2}} \pm \frac{1}{2} \left(1 - \frac{eV(r)}{E_0} - \frac{I_+}{I_r} \right)^{\frac{1}{2}} - \frac{N_e(\infty)}{N_+(\infty)} e^{eV(r)/kT_e} - \frac{N_-(\infty)}{N_+(\infty)} e^{eV(r)/kT_-} \right]. \quad (2.21)$$

In this equation, the plus sign is used for $r \geq r_0$, and the minus sign is used for $r \leq r_0$, where r_0 is defined by equations (2.15). Also, the current I_r is given by Eq. (2.16), and I_+ is given by Eq. (2.20).

2.2 NUMERICAL TECHNIQUES

Poisson's equation, Eq. (2.21), describes the potential distribution in the vicinity of a contaminant in a plasma. The effects of angular momentum have been included. This equation does not lend itself readily to analytic solutions. The next paragraphs will describe the numerical techniques employed in solving Eq. (2.21). In all cases discussed in this chapter, the following assumptions are held constant: the positive and negative ion temperatures are equal, and that their masses are equal, being the mass of singly ionized argon atoms, $M = 39.44m_p$, where m_p is the rest mass of a proton. The choice of equal positive and negative ion masses is completely arbitrary, and are chosen equal only as a matter of convenience. Other choices for masses will only scale the results discussed in this chapter.

2.2.1 Normalized Equations

An important step in solving this equation was to simplify it through the use of normalized variables. These normalized variables are as follows:

$$x = \frac{a}{r} \left(\frac{kT_e M_+ 4}{E_0 M_- \pi} \right)^{\frac{1}{2}} \left(\frac{N_e}{N_+} e^{eV_0/kT_e} + \frac{N_-}{N_+} \left(\frac{T_- m_e}{T_e M_-} \right)^{\frac{1}{2}} e^{eV_0/kT_-} \right)^{\frac{1}{2}}, \quad (2.22)$$

$$y = \frac{-eV(r)}{E_0}, \quad (2.23)$$

$$\lambda = \frac{\left(\frac{N_e}{N_+} \right) \left(\frac{\lambda_D}{a} \right)^2 \left(\frac{E_0}{kT_e} \right)^{\frac{3}{2}} \left(\frac{m_e \pi}{M_+ 4} \right)^{\frac{1}{2}}}{\frac{N_e}{N_+} e^{eV_0/kT_e} + \frac{N_-}{N_+} \left(\frac{T_- m_e}{T_e M_-} \right)^{\frac{1}{2}} e^{eV_0/kT_-}}, \quad (2.24)$$

$$\beta = \frac{E_0}{kT_e}, \quad (2.25)$$

$$\beta_- = \frac{E_0}{kT_-}, \quad (2.26)$$

and

$$\alpha = \frac{N_e}{N_+}. \quad (2.27)$$

The quantity λ_D represents the Debye length of the plasma. The quantities N_+ , N_e , and N_- represent the number densities in the bulk region of the plasma (i.e. $r = \infty$). Substituting equations (2.22-2.27) into Eq. (2.21) yields the following form of Poisson's equation:

$$\lambda x^4 \frac{d^2 y(x)}{dx^2} = \frac{1}{2} (1+y)^{\frac{1}{2}} \pm \frac{1}{2} (1+y-x^2)^{\frac{1}{2}} - \alpha e^{-\beta y} - (1-\alpha) e^{-\beta_- y}. \quad (2.28)$$

The plus sign is used when $x \leq x_0$, and the minus sign is used when $x \geq x_0$. Note that $x \propto \frac{1}{r}$, therefore, x decreases away from the contaminant, and $x = 0$ corresponds to the bulk plasma region $r = \infty$. The ordinate, x_0 , is defined by equations (2.15) when the normalized variables are substituted. The equations (2.15) become

$$1 + y(x_0) - x_0^2 = 0, \quad (2.29a)$$

$$\frac{d}{dx} (1 + y(x) - x^2)_{x=x_0} = 0. \quad (2.29b)$$

2.2.2 Boundary Conditions and Constraints

Two boundary conditions are required for the second order Poisson differential equation (Eq. (2.28)). These boundary conditions are readily available at a single point x_0 as defined by equations (2.29). Having both boundary conditions defined at one point is fortuitous in light of using a self-starting integration algorithm such as the Runge-Kutta-Nyström method [8]. However, the problem is still incompletely specified. Both λ , and x_0 are unknown. The parameters such as α , β , and β_- are arbitrary, and are dependent on the chosen plasma parameters. Both the voltage at the contaminant and the relationship of this voltage to the contaminant size are unknown. Therefore, two other constraints are required.

The first constraint is clearly that the voltage must vanish at an infinite radius. Unfortunately, specifying boundary conditions at infinity is not practical for numerical purposes. This boundary condition provided the motivation for defining the normalized radius x to be inversely proportional to r , so that the boundary condition at infinite radius becomes a boundary condition at $x = 0$. Specifically,

$$y(0) = 0. \tag{2.30}$$

The second constraint is not so obvious. Notice that the boundary conditions of equations (2.29) specify that the solution to Poisson's equation be tangent to the curve

$$y = x^2 - 1$$

at the point x_0 . Furthermore, the quantity $1 + y - x^2$ appears under a square root in the right side of Eq (2.28). Therefore, in order to obtain real solutions to Poisson's equation, this quantity must always be positive. In other words, the solution must always lie above and to the left of the curve $y = x^2 - 1$. (See Fig. 2.8.) For this to be true, the curvature of the solution at x_0 must be greater than or equal to that of the curve $y = x^2 - 1$. Since the curvature is inversely proportional to the second derivative, this places a lower bound on the value of the second derivative of y at

x_0 , that bound being the second derivative of $x^2 - 1$, or the value 2. Therefore, evaluating Eq. (2.28) at x_0 , and using the lower bound on the second derivative, an upper bound on lambda is obtained, namely

$$\lambda \leq \frac{\frac{x_0}{2} - \alpha e^{-\beta(x_0^2-1)} - (1-\alpha)e^{-\beta-(x_0^2-1)}}{2x_0^4}. \quad (2.31)$$

Plots of Eq. (2.31) (with the equal sign) are shown in Fig 2.6. The effects of α and β are shown. For an α of 1.00 (no negative ions), the curves are strongly dependent on β , the ratio of positive ion and electron energies. As negative ions are introduced, the number density of electrons decreases, and the dependence of the curves on β disappears. This is seen in figures 2.6b and 2.6c as α decreases. Only positive values of λ are allowed since, by Eq. (2.24), λ must be greater than zero.

2.2.3 Strategy of Integration

These four constraints, namely equations (2.29a), (2.29b), (2.30), and (2.31), now completely define the problem. The task now is to determine how to apply these constraints to solve the problem. To begin with, the Runge-Kutta-Nyström technique is self-starting, and so it requires two boundary conditions at a starting point. Therefore, equations (2.29) are used as the starting criteria for the numerical integrator. The point x_0 is initially chosen arbitrarily, as is a value of λ subject to the constraints of Eq. (2.31).

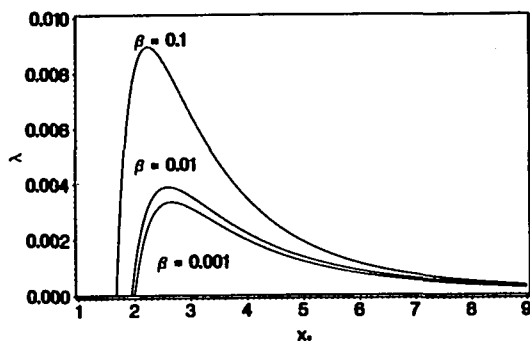
The next step is to begin the integration and proceed toward the origin, in the direction of decreasing x . Application of Eq. (2.30) should be useful in determining if the proper choice of x_0 and λ have been made. Unfortunately, in implementing Poisson's equation numerically, it is necessary to rewrite Eq. (2.28) such that only the second derivative remains on the left side of the equation. Therefore, the right hand side is divided by λx^4 , and as x approaches zero, the second derivative increases without bound. This unbounded behavior is a numerical limitation and not a physical one. As a result, it is not possible to carry the integration through the origin.

What can be done, however, is to iterate on the choice of λ , holding x_0 fixed, to obtain a solution that approaches closest to the origin before diverging. Such iterations on λ have been consistently found to converge to a value equal to the upper bound defined by Eq. (2.31). (It is not clear why this should be so.) Consequently, the constraints given in equations (2.30) and (2.31) reduce to a single defining relationship between x_0 and λ . In terms of solving Poisson's equation, once an arbitrary choice for x_0 is made, the value of λ is given by the equality of Eq. (2.31). Choosing x_0 arbitrarily is analogous to choosing a , the size of the contaminant to be investigated.

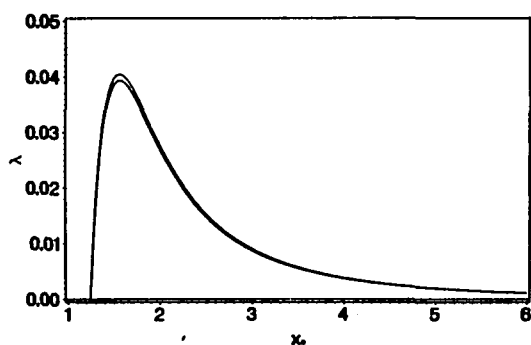
Once a value of x_0 has been chosen, and the corresponding λ calculated, it only remains to perform the integration in the direction of increasing x . This is the direction in which the radius r decreases and approaches that of the contaminant, a . It is now necessary to determine a stopping criterion for the integration. The integration should stop when the radius of the particle is reached, that is, when $r = a$. The stopping criterion then becomes Eq. (2.22), with $r = a$. If y_a is defined as the value of y corresponding to V_a , the contaminant voltage, then, in terms of the other normalized parameters in equations (2.23) to (2.27), Eq. (2.22) becomes

$$x_a = \left(\frac{M_+}{M_-} \frac{4}{\pi\beta} \right)^{\frac{1}{4}} \left(\alpha e^{-\beta y_a} + (1 - \alpha) \left(\frac{\beta}{\beta_-} \frac{m_e}{M_-} \right)^{\frac{1}{2}} e^{-\beta_- y_a} \right)^{\frac{1}{2}}. \quad (2.32)$$

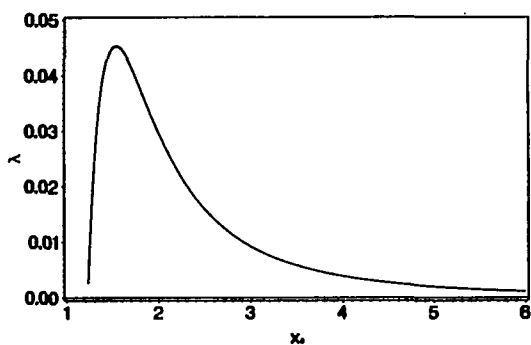
The dependence between x_a and y_a as defined by Eq. (2.32) is shown graphically in Fig. 2.7. As in all cases discussed in this chapter, these plots are generated under the assumptions that the positive and negative ion temperatures are equal, and that their masses are equal, being the mass of singly ionized argon atoms, $M = 39.44m_p$, where m_p is the rest mass of a proton. Also plotted in each figure is the curve $y = x^2 - 1$. As mentioned above, the solution to Poisson's equation must lie above and to the left of this curve. Therefore, only values of x and y in this region are possible as solutions to Eq. (2.28). The solutions for Eq. (2.32) lie on the curves labeled by the respective values of β . Therefore, a solution to Poisson's equation must terminate on one member of this family of curves.



(a)

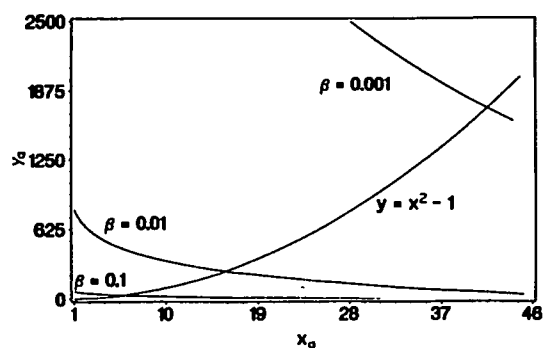


(b)

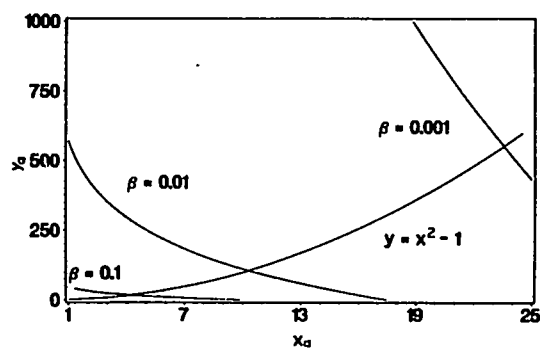


(c)

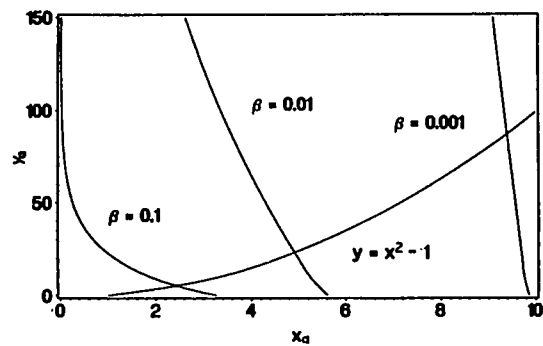
Fig. 2.6 Plots of Eq. (2.31), showing the relationship between x_0 and λ . The positive and negative ion energies are assumed to be equal ($\beta_- = 1.0$). (a) $\alpha = 1.00$. (b) $\alpha = 0.10$. Note the shift in the peak to lower x . This plot is also for the same three values of β as in (a), but the lower two curves become indistinguishable on this scale. (c) $\alpha = 0.01$. All three curves have become indistinguishable.



(a)



(b)



(c)

Fig. 2.7 Plots of Eq. (2.32), showing the stopping criterion for the integration for different values of α and β . Also shown is the curve $x^2 - 1$. All solutions to Poisson's equation must lie above and to the left of this curve. For all curves, $\beta_- = 1.0$. The intersections of the curves of Eq. (2.32) with the curve $x^2 - 1$ define upper limits on x . (a) $\alpha = 1.00$. (b) $\alpha = 0.10$. (c) $\alpha = 0.01$.

There are some important characteristics of these curves that need to be mentioned. First, note that based on the curves of Fig. 2.6, x_a cannot be less than the zero for the curve of $\lambda(x_0)$. Furthermore, $y < 0$ is a non-physical solution.

Most importantly, and most surprisingly, the intersection of the curve $y = x^2 - 1$ with the curve $y_a(x)$ defines a maximum x_a . This corresponds to a minimum contaminant radius. That is, there is a minimum radius for which this analysis is valid. For contaminants with radii less than this radius a different approach must be used. Therefore, this radius has been given the name a_{crit} . For a discussion of particles with radii less than a_{crit} see chapter 3.

2.2.4 Conversion to Physical Parameters

A complete solution to Poisson's equation in the normalized form can now be obtained using the techniques discussed above. It now remains to relate the normalized solution to a physical one. The first step is to find y_a from the terminating point of the solution as defined by Eq. (2.32), and then to find V_a from Eq. (2.23). The value of a can then be found from the definition of λ given in Eq. (2.24). Finally, the values of x can now be converted to values of r using the values of V_a and a just found, and the solution is complete.

2.3 RESULTS

The results of the calculations discussed above will now be presented. First, a discussion of the critical contaminant radius will be given. Next, the criteria for starting an integration will be discussed as the relation between the choice of x_0 and the contaminant radius will be evaluated. Then results regarding the voltage, flux density, contaminant charge, and the electric field will be presented and interpreted.

2.3.1 Critical Contaminant Radius

As mentioned in connection with Fig. 2.7, the intersection of the curve $y_a(x_a)$ with the curve $y = x^2 - 1$ defines a maximum x for which Poisson's equation holds.

A solution to Poisson's equation for the case where the solution contains the point of intersection is shown in Fig. 2.8. Considering the various solutions for different values of α and β leads to the curves shown in Fig. 2.9a. As in all results discussed in this chapter, these curves were generated with the following parameters held constant.

$$N_+ = 10^{10} \text{ cm}^{-3},$$

$$T_- = 0.0258 \text{ eV},$$

$$E_0 = 0.0258 \text{ eV},$$

and

$$M_+ = M_- = 39.44m_p.$$

Other constants (*e.g.* π , k) have their usual values as well. For comparison, the Debye length is plotted in Fig. 2.9b. Note that the critical radius is typically smaller than the Debye length, although for some cases it may be as large as the Debye length.

The curves of Fig. 2.9a show a striking dependence on the negative ions. In the absence of negative ions ($\alpha = 1.0$), the critical radius decreases with increasing β , whereas when negative ions are present, the curves increase with β .

2.3.2 Choosing x_0

As mentioned above, the choice for x_0 is arbitrary. It is analogous to choosing the size of the contaminant to be investigated. The relationship between x_0 and a is shown in Fig. 2.10. These figures were generated by first arbitrarily choosing values for x_0 , performing the integration of Poisson's equation, and then determining the value of a arrived at. Now that curves of x_0 versus a have been generated in this manner, it is possible to proceed in the opposite manner. Namely, a can now be chosen first, and the appropriate x_0 can be determined from the curves of Fig. 2.10. Figure 2.6 and Eq. (2.31) were used to associate the chosen values of x_0 with a suitable λ . The ranges of the x_0 axes in Fig. 2.10 are bound on the lower

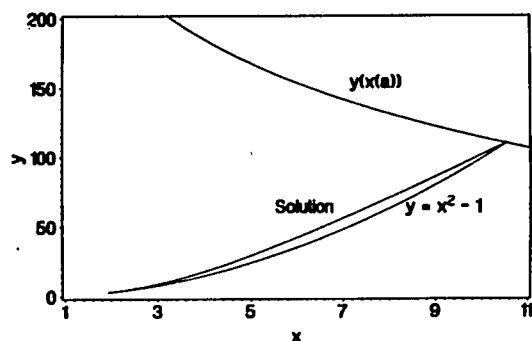
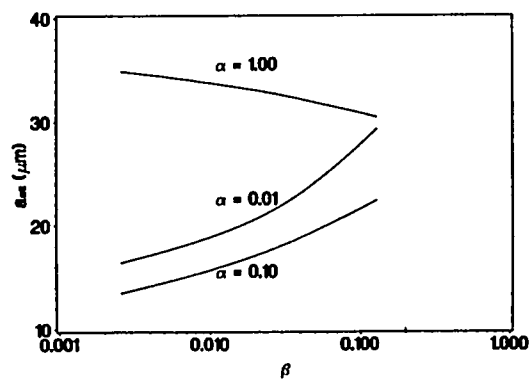
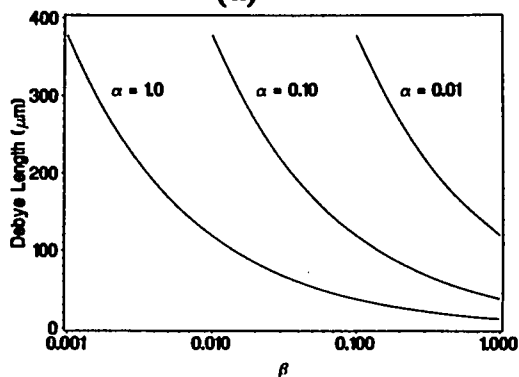


Fig. 2.8 A typical solution to Poisson's equation. $\alpha = 1.0$, $\beta = 0.0258$, $\beta_- = 1.0$. The solution shown corresponds to the conditions defining the critical contaminant radius.

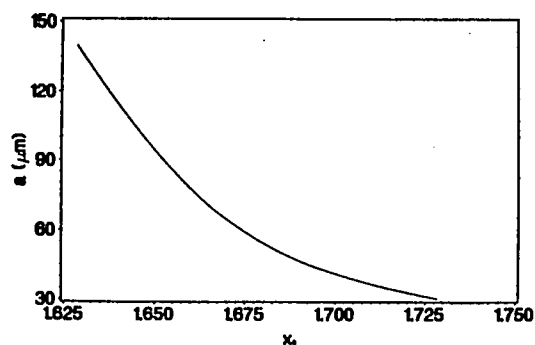


(a)

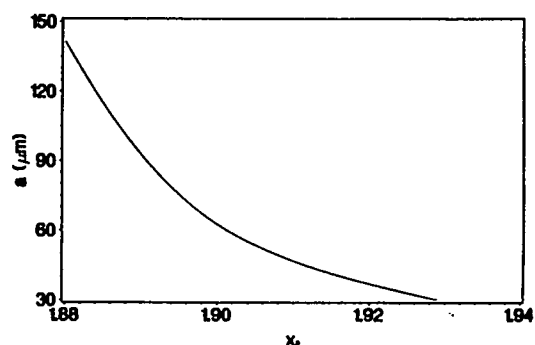


(b)

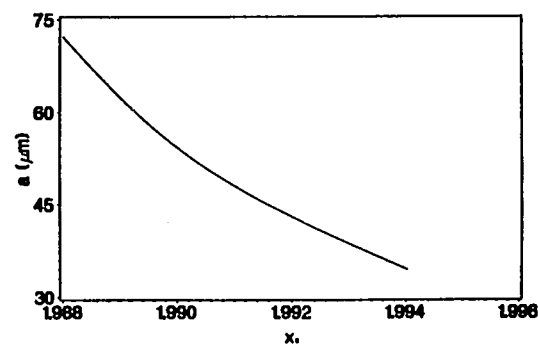
Fig. 2.9 (a) Dependence of the critical contaminant radius on α and β . $N_+ = 10^{10} \text{ cm}^{-3}$, $T_+ = 0.0258 \text{ eV}$, $T_- = 0.0258 \text{ eV}$. (b) The Debye length, shown for comparison.



(a)

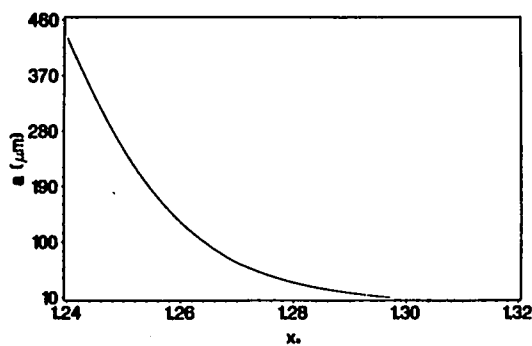


(b)

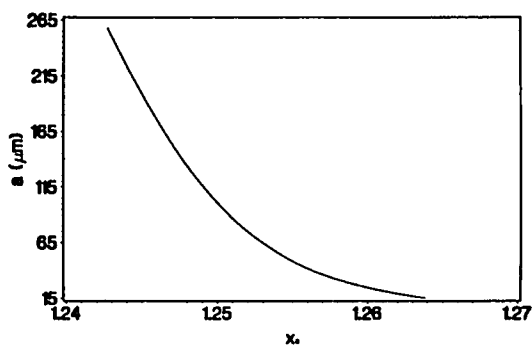


(c)

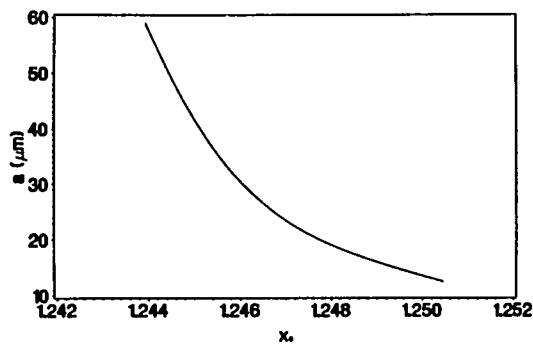
Fig. 2.10 Graphs showing the dependence of a on x_0 for various values of N_e and T_e . The x axes in the following plots are limited on the lower end by the zeros of Eq. (2.31), and on the upper end by a_{crit} . $N_+ = 10^{10} \text{ cm}^{-3}$, $T_+ = 0.0258 \text{ eV}$, $T_- = 0.0258 \text{ eV}$. (a) $N_e = 10^{10} \text{ cm}^{-3}$, $T_e = 0.2 \text{ eV}$. (b) $N_e = 10^{10} \text{ cm}^{-3}$, $T_e = 1.0 \text{ eV}$. (c) $N_e = 10^{10} \text{ cm}^{-3}$, $T_e = 10.0 \text{ eV}$.



(d)

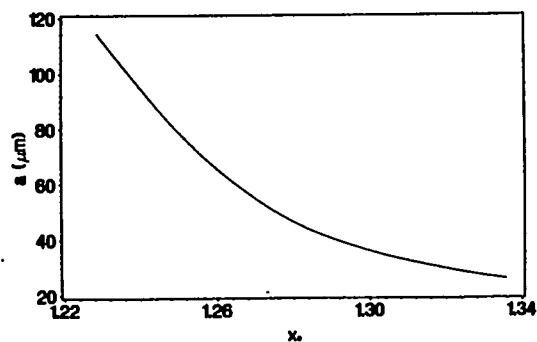


(e)

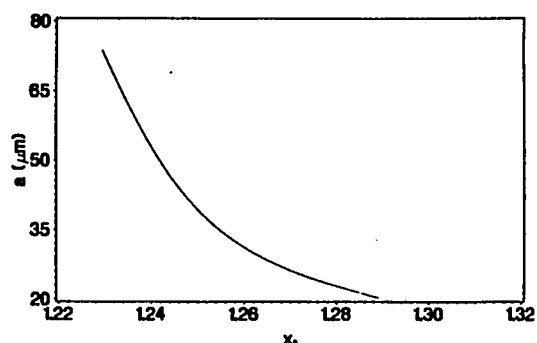


(f)

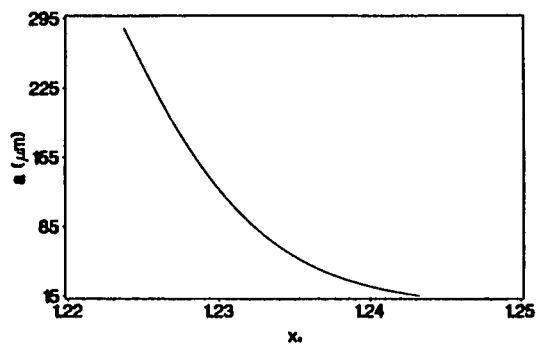
Fig. 2.10 Graphs showing the dependence of a on x_0 for various values of N_e and T_e . The x axes in the following plots are limited on the lower end by the zeros of Eq. (2.31), and on the upper end by a_{crit} . $N_+ = 10^{10} \text{ cm}^{-3}$, $T_+ = 0.0258 \text{ eV}$, $T_- = 0.0258 \text{ eV}$. (d) $N_e = 10^9 \text{ cm}^{-3}$, $T_e = 0.2 \text{ eV}$. (e) $N_e = 10^9 \text{ cm}^{-3}$, $T_e = 1.0 \text{ eV}$. (f) $N_e = 10^9 \text{ cm}^{-3}$, $T_e = 10.0 \text{ eV}$.



(g)



(h)



(i)

Fig. 2.10 Graphs showing the dependence of a on x_0 for various values of N_e and T_e . The x axes in the following plots are limited on the lower end by the zeros of Eq. (2.31), and on the upper end by a_{crit} . $N_+ = 10^{10} \text{ cm}^{-3}$, $T_+ = 0.0258 \text{ eV}$, $T_- = 0.0258 \text{ eV}$. (g) $N_e = 10^8 \text{ cm}^{-3}$, $T_e = 0.2 \text{ eV}$. (h) $N_e = 10^8 \text{ cm}^{-3}$, $T_e = 1.0 \text{ eV}$. (i) $N_e = 10^8 \text{ cm}^{-3}$, $T_e = 10.0 \text{ eV}$.

end by the zeros of Eq. (2.31), and on the upper end by a_{crit} . This upper limit on x_0 interestingly restricts the ranges to lie to the left of the maxima of Eq. (2.31) (see Fig. 2.6).

2.3.3 Voltage Characteristics

Figure 2.11 shows several typical solutions to Poisson's equation along with the two limiting curves $y(x(a))$ and $y = x^2 - 1$. Three cases are shown, corresponding to different values of a (or, equivalently, different values of x_0 and λ). The third case, Case 3, corresponds to the critical radius conditions, and the other two cases correspond to arbitrary choices of x_0 (or a). The values of x_0 are indistinguishable on the horizontal scale shown, so the values of λ corresponding to each solution are shown.

Using the knowledge of λ , x_a , and $y(x_a)$, these normalized solutions can be transformed to solutions in terms of the physical variables. These physical solutions are shown in Fig. 2.12. These curves show the potential distribution as a function of radius from the particle. Note that the voltages are negative as expected, and they decay considerably within $100 \mu m$ of the contaminant. The curves terminate on the left side at the contaminant, and on the right side at the radius r_0 .

Considering other solutions similar to those in Fig. 2.12 for various cases of α , and β , the dependence of the contaminant voltage on the contaminant radius for the various cases can be determined. The results of these investigations are shown in Fig. 2.13. The voltage at the surface of the contaminant is weakly dependent on the contaminant size, although there is a slight increase in voltage as the contaminant size increases, as expected. On the other hand, the voltage shows a strong dependence on the electron energy. As the electron energy increases (β decreases) the contaminant develops a larger voltage. This supports the intuition that the larger voltage is needed to repel the higher energy electrons to maintain flux equilibrium. Furthermore, a decrease in the number density of the electrons (α decreases) causes a decrease in the magnitude of the voltage as well. The sensitivity to a seems to increase a little as α decreases. However, the overall sensitivity

to the presence of negative ions is small, requiring very large numbers of negative ions to produce significant effects.

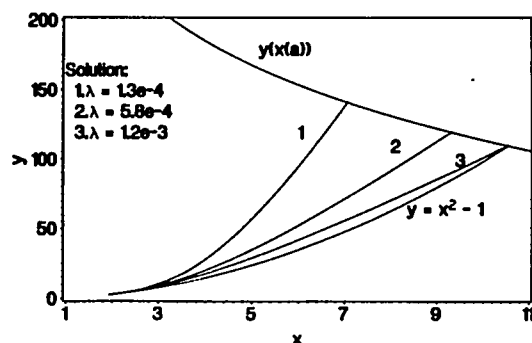


Fig. 2.11 Typical normalized solutions for several general cases. $\alpha = 1.00$, $\beta = 0.0258$, $\beta_- = 1.0$.

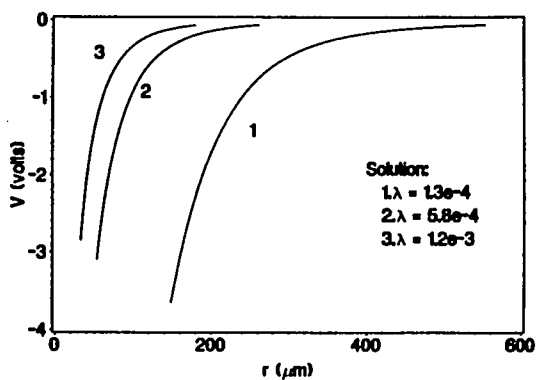
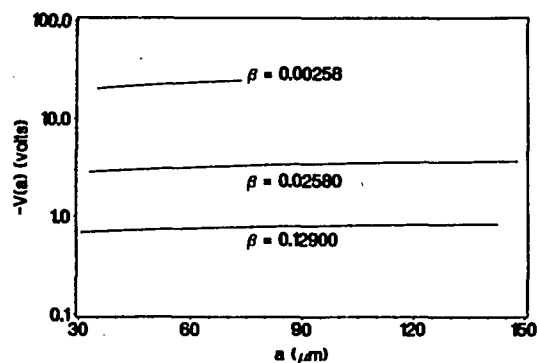
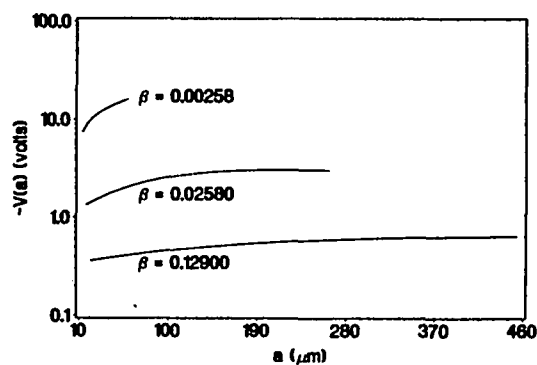


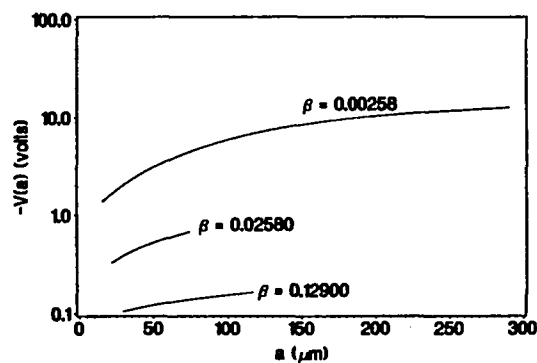
Fig. 2.12 Typical physical solutions for the same cases as in Fig. 2.11. The curves terminate on the right at r_0 , and on the left at a . $\alpha = 1.00$, $\beta = 0.0258$, $\beta_- = 1.0$, $N_+ = 10^{10} \text{ cm}^{-3}$, $T_+ = 0.0258 \text{ eV}$, $T_- = 0.0258 \text{ eV}$.



(a)



(b)



(c)

Fig. 2.13 The dependence of the contaminant voltage on a , α and β . $N_+ = 10^{10} \text{ cm}^{-3}$, $T_+ = 0.0258 \text{ eV}$, $T_- = 0.0258 \text{ eV}$. (a) $\alpha = 1.00$. (b) $\alpha = 0.10$. (c) $\alpha = 0.01$. Curves terminate on the left at a_{crit} .

2.3.4 Flux Characteristics

Once the voltage at the surface of the contaminant is found, other important parameters such as the particulate flux to the surface, the contaminant charge, and the electric field can be found as well. The flux density of positive charges to the surface can be found from Eq. (2.20) by dividing I_+ by $4\pi a^2 e$. Since this flux is equal to that of the negative charges, the total flux is simply twice that given by Eq. (2.20).

Plots of $\Gamma_+ = I_+/4\pi a^2 e$ (Eq. (2.20)) for various values of α and β (with the corresponding values of V_a) are shown in Fig. 2.14. Qualitatively, the curves are similar to the voltage curves of Fig. 2.13. The flux shows a slight inverse dependence on the contaminant size, as predicted by the formula $\Gamma_+ = I_+/4\pi a^2 e$. Also, an increase in electron energy leads to an increase in particulate flux to the contaminant surface. This increase occurs in spite of the increase in voltage to repel the negative charges. Furthermore, a decrease in the number density of electrons also causes a decrease in the particulate flux to the contaminant. But, as noted in connection with the voltage characteristics, it takes a very large decrease in the electron number density (meaning a corresponding large increase in the number density of negative ions) to produce significant effects.

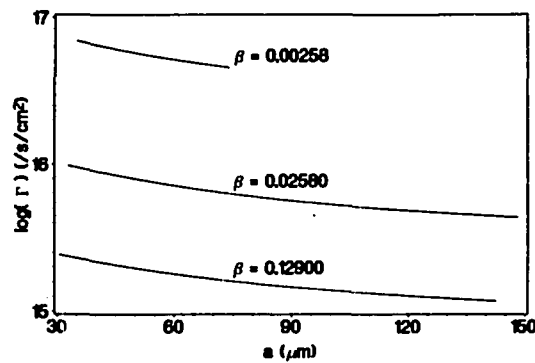
2.3.5 Electric Field Characteristics

As part of the solution for Poisson's equation, the first and second derivatives of the voltage must be calculated. The electric field is directly related to the first derivative of the voltage as

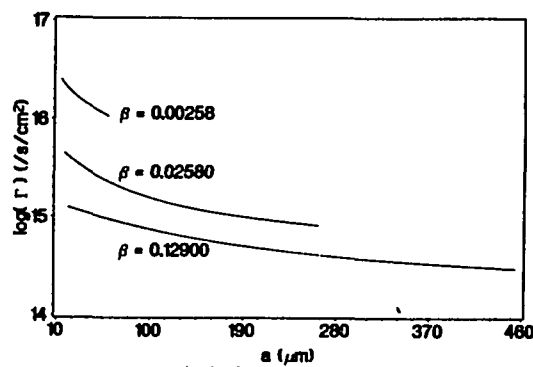
$$E = -\frac{dV}{dr}.$$

Typical solutions for the electric field for the same conditions as in Fig. 2.12 are shown in Fig. 2.15. As with the voltage, the electric field decays significantly within $100 \mu m$ of the contaminant.

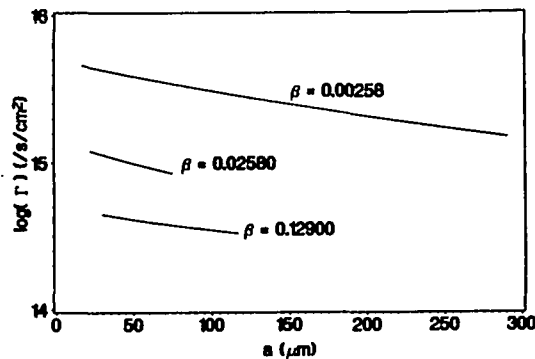
Extracting information about the electric field at the surface of the contaminant from several solutions as shown in Fig. 2.15 for various values of α and β ,



(a)



(b)



(c)

Fig. 2.14 The flux density of one species of charged particles to the surface of the contaminant. The flux density of positive charges is equal to the flux density of negative charges. The total flux density is twice the value given by these curves. Curves terminate on the left at a_{crit} . $N_+ = 10^{10} cm^{-3}$, $T_+ = 0.0258 eV$, $T_- = 0.0258 eV$. (a) $\alpha = 1.00$. (b) $\alpha = 0.10$. (c) $\alpha = 0.01$.

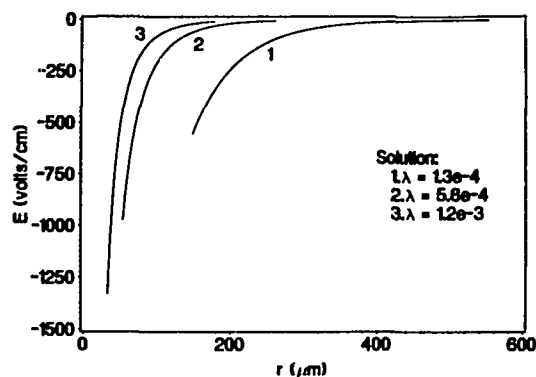


Fig. 2.15 Typical electric field distributions for the same cases as in Fig. 2.11 and Fig. 2.12. $\alpha = 1.00$, $\beta = 0.0258$, $\beta_- = 1.0$, $N_+ = 10^{10} \text{ cm}^{-3}$, $T_+ = 0.0258 \text{ eV}$, $T_- = 0.0258 \text{ eV}$.

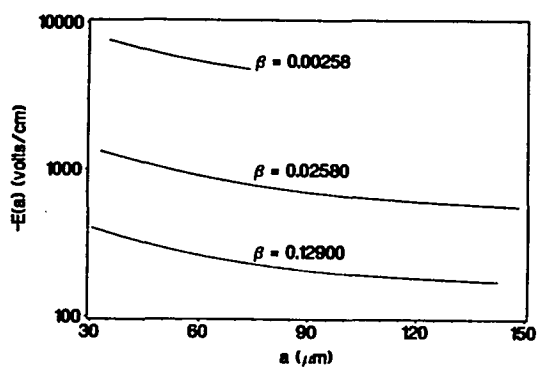
yields the results shown in Fig. 2.16. Again, these curves are quite similar qualitatively to the voltage and flux characteristics. Larger electron energies force the contaminant to develop larger electric fields. Furthermore, larger particles tend to develop a slightly weaker field. The electric field also decreases slightly as the number density of electrons decreases greatly.

2.3.6 Charge Characteristics

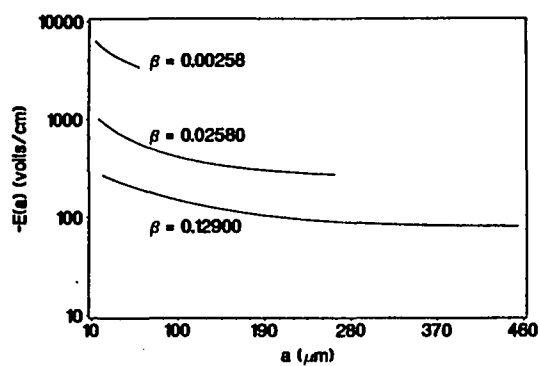
The charge on the contaminant can be evaluated using the relationship between the charge and electric field as defined by the Coulomb force. The charge Q is related to the electric field E as follows:

$$Q = \frac{E}{4\pi\epsilon_0 a^2}.$$

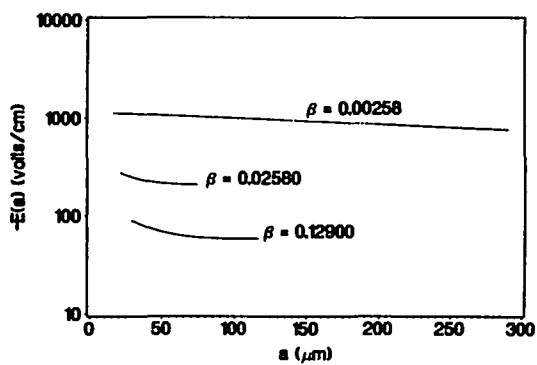
Plots of contaminant charge versus contaminant radius are shown in Fig. 2.17. For a typical case where $\alpha = 1$, $\beta = 0.0258$, and $a = a_{crit} = 33 \mu\text{m}$, the contaminant supports a charge of about 1.6×10^{-14} coulombs. This corresponds to nearly 10^5 electrons residing on the surface of the contaminant. Again, the dependence on the number density of the negative ions is weak. It is interesting to note that the



(a)

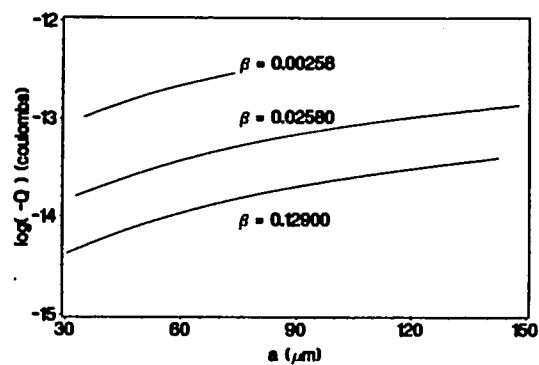


(b)

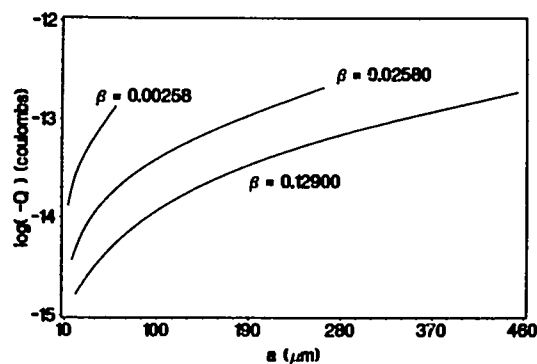


(c)

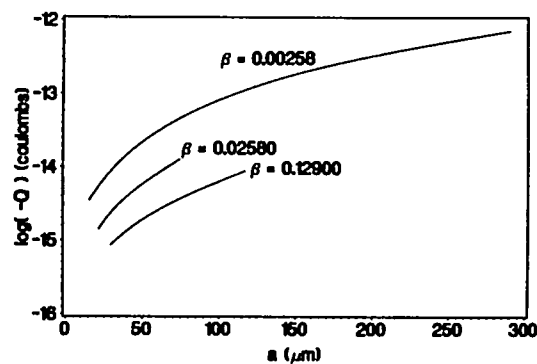
Fig. 2.16 The electric field at the surface of the contaminant. $N_+ = 10^{10} \text{ cm}^{-3}$, $T_+ = 0.0258 \text{ eV}$, $T_- = 0.0258 \text{ eV}$. (a) $\alpha = 1.00$. (b) $\alpha = 0.10$. (c) $\alpha = 0.01$. Curves terminate on the left at a_{crit} .



(a)



(b)



(c)

Fig. 2.17 The dependence of the contaminant charge on a , α and β . $N_+ = 10^{10} \text{ cm}^{-3}$, $T_+ = 0.0258 \text{ eV}$, $T_- = 0.0258 \text{ eV}$. (a) $\alpha = 1.00$. (b) $\alpha = 0.10$. (c) $\alpha = 0.01$. Curves terminate on the left at a_{crit} .

contaminant charge shows a much stronger dependence on a than do the voltage, flux, and electric field.

2.4 SUMMARY

In this chapter, the effects of the charge density distribution including angular momentum have been developed and incorporated into Poisson's equation. Integration of Poisson's equation yielded information about the contaminant's voltage, charge, surface flux density, and electric field. The effects of electron energy and electron number density on each of these parameters has been investigated. It has also been pointed out that the presence of negative ions only becomes significant when their numbers become very large, approaching the number of positive ions.

Most importantly, in this chapter, it was shown that there is a critical contaminant radius a_{crit} , below which Poisson's equation breaks down. This radius is strikingly large, being about the same order of magnitude as the Debye length. Typically, a_{crit} ranges from about $10 \mu m$ to almost $40 \mu m$. Contaminants with radii of this magnitude are extremely large by today's semiconductor processing standards. Clean processes are usually concerned with contaminants of a much smaller size, a couple of microns down to sub-micron contaminants. Therefore, the next chapter develops a theory that is suitable for very small particles.

Chapter 3

Coulomb Model

3.1 THEORY

In this chapter, an analysis of the Coulomb force as a central force will be used to determine the characteristics of the environment surrounding a contaminant whose radius is considerably smaller than the Debye length. The equations describing the trajectory of a particle influenced by the contaminative forces will be derived from considering the form of Newton's second law in polar coordinates. Then, the flux densities of the particles to the surface of the contaminant will be developed from consideration of the conservation of energy and the limits of integration in the flux integrals. Finally, the significant results of these calculations will be presented and interpreted.

3.1.1 Justification

The justification for considering the validity of a central Coulomb force model in a plasma environment stems from two observations. First, and most significantly, as was seen in the last chapter, Poisson's equations break down below a radius a_{crit} . This radius is of the order, but less than the Debye length. Poisson's equation breaks down because the charge density distribution is no longer meaningful in describing the characteristics of the environment. This is because the average separation of charged particles is comparable to the size of the contaminant. Furthermore, since the contaminants' radii being considered are considerably smaller than the Debye length, the potential developed in the vicinity of the contaminant will not be significantly altered by the plasma. The spatial extent of the perturbations will only be on the order of the Debye length.

3.1.2 Central Force Equations

For contaminants with $r \ll a_{crit} < \lambda_D$, a central force analysis can be done to determine the voltage ($V(a)$) and charge (Q) on the contaminant. The force the contaminant exerts on a particle of charge q is the Coulomb force,

$$\begin{aligned} \mathbf{F} &= \frac{Qq}{4\pi\epsilon_0 r^2} \hat{\mathbf{r}} \\ &= \frac{K}{r^2} \hat{\mathbf{r}}. \end{aligned} \quad (3.1)$$

In this equation, K is defined as

$$K = \frac{Qq}{4\pi\epsilon_0}.$$

The magnitude of the charge on the particle is e . Therefore, $q = \pm e$, depending on whether the particle is a positive ion or an electron. In chapter 2 it was shown that the flux of negative ions to the surface of the contaminant would be negligibly small. Therefore, here their flux will be neglected. Furthermore, the charge on the contaminant is negative as described in the previous chapter ($Q < 0$). The system, particle+contaminant, is depicted in Fig. 3.1. It is known from Newton's second law that the force on the particle is also given by

$$\mathbf{F} = m\mathbf{a}. \quad (3.2)$$

(Bold symbols represent vector quantities. "Hatted" symbols represent unit vectors.)

Comparing Eq. (3.2) with Eq. (3.1), it is clear that there is only a radial component of acceleration, thus

$$\mathbf{a} = a_r \hat{\mathbf{r}}. \quad (3.3)$$

If the particle is at a position $\mathbf{r} = r\hat{\mathbf{r}}$ and has a velocity \mathbf{v} as shown in Fig. 3.1, then the acceleration can be written as $\mathbf{a} = \ddot{\mathbf{r}} = \dot{\mathbf{v}}$, where the dots indicate time derivatives. Now the velocity is the time derivative of

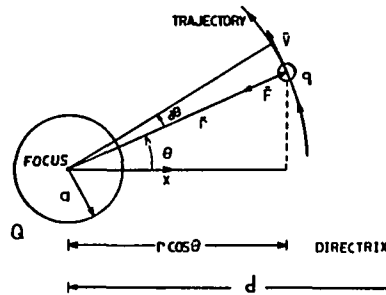


Fig. 3.1 A particle under the influence of a central force travels along a conic section trajectory that can be described by the particle's distance from both the directrix and the focus.

the vector \mathbf{r} , which by the chain rule for differentiation can be written as

$$\mathbf{v} = \frac{d\mathbf{r}}{dt} = \frac{dr}{dt} \hat{\mathbf{r}} + r \frac{d\hat{\mathbf{r}}}{dt}.$$

It is necessary, therefore, to determine how the unit vectors change with time. Figure 3.2 shows how the polar coordinate system would rotate in time dt as the particle moves through the angle $d\theta$ shown in Fig. 3.1. From Fig. 3.2, it is clear that

$$\begin{aligned} d\hat{\mathbf{r}} &= d\theta \hat{\boldsymbol{\theta}} \\ d\hat{\boldsymbol{\theta}} &= -d\theta \hat{\mathbf{r}}. \end{aligned}$$

The time rate of change in the unit vectors is found by dividing both expressions by dt . Therefore,

$$\begin{aligned} \frac{d\hat{\mathbf{r}}}{dt} &= \frac{d\theta}{dt} \hat{\boldsymbol{\theta}} \\ \frac{d\hat{\boldsymbol{\theta}}}{dt} &= -\frac{d\theta}{dt} \hat{\mathbf{r}}. \end{aligned}$$

Using these expressions in the equation for \mathbf{v} above, and reverting back to the dot notation, the velocity is given by,

$$\mathbf{v} = \dot{r} \hat{\mathbf{r}} + r \dot{\theta} \hat{\boldsymbol{\theta}}. \quad (3.4)$$

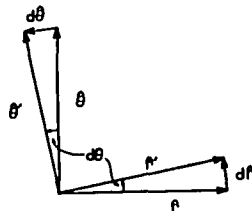


Fig. 3.2 How the unit vectors change as they rotate through an infinitesimal angle.

Differentiating again gives the following expression for the acceleration,

$$\mathbf{a} = (\ddot{r} - r\dot{\theta}^2)\hat{\mathbf{r}} + (r\ddot{\theta} + 2\dot{r}\dot{\theta})\hat{\boldsymbol{\theta}}. \quad (3.5)$$

Therefore, from Eq. (3.3),

$$(\ddot{r} - r\dot{\theta}^2) = a_r \quad (3.6)$$

$$(r\ddot{\theta} + 2\dot{r}\dot{\theta}) = 0. \quad (3.7)$$

Now, by equations (3.6), (3.2) and (3.1), then

$$m\ddot{r} - mr\dot{\theta}^2 = \frac{Qq}{4\pi\epsilon_0 r^2} = \frac{K}{r^2}. \quad (3.8)$$

Furthermore, note that when Eq. (3.7) is multiplied by r , it reduces to $\frac{d}{dt}(r^2\dot{\theta}) = 0$, which has the solution $r^2\dot{\theta} = \text{a constant}$. The quantity $mr^2\dot{\theta}$ can be shown to be the angular momentum of the particle. The angular momentum is defined as the moment of linear momentum about the focus:

$$\begin{aligned} \mathbf{J} &= \mathbf{r} \times m\mathbf{v} \\ &= r\hat{\mathbf{r}} \times m(\dot{r}\hat{\mathbf{r}} + r\dot{\theta}\hat{\boldsymbol{\theta}}) \\ &= mr^2\dot{\theta}\hat{\mathbf{z}}. \end{aligned}$$

Therefore,

$$r^2\dot{\theta} = \frac{J}{m} = \text{constant}. \quad (3.9)$$

Now by making the substitution $u = \frac{1}{r}$ in Eq. (3.8), and using the result above, Eq. (3.8) can be written as

$$\frac{d^2u}{d\theta^2} + u = -\frac{Km}{J^2}.$$

(The minus sign on the right side of this equation is the result of differentiating $1/u$.) This equation has the solution

$$u = \frac{1}{r} = C \cos \theta - \frac{Km}{J^2}, \quad (3.10)$$

where C is a constant. (A more general solution would include a coordinate rotation term, θ' , in the cosine term, but the coordinate system has been chosen here such that $\theta' = 0$.)

It is interesting to note that Eq. (3.10) is of the same form as the general equation for a conic section. A conic section trajectory is one whose ratio of the distance from a point (the focus) to the distance from a line (the directrix; see Fig. 3.1), known as the eccentricity f , is a constant. That is,

$$f = \frac{r}{d - r \cos \theta},$$

or

$$\frac{1}{r} = \frac{1}{d} \cos \theta + \frac{1}{fd}. \quad (3.11)$$

Comparing equations (3.10) and (3.11), The parameters d and f of the trajectory can be determined as follows:

$$d = \frac{1}{C},$$

and

$$f = -\frac{CJ^2}{Km}. \quad (3.12)$$

It is the eccentricity, f , that determines the type of trajectory the particle will follow. Namely, if $f < 1$, the trajectory is an ellipse; if $f = 1$, the trajectory is a parabola; and if $f > 1$, the trajectory is a hyperbola.

3.1.3 Conservation of Energy

In order to determine the magnitude of f for the system of Fig. 3.1, the conservation of energy must be considered. Let E be the total energy of the particle, T the kinetic energy, and U the potential energy. Then energy is conserved if $E = T + U$. The kinetic energy is given by

$$T = \frac{1}{2}m|\mathbf{v}|^2 = \frac{1}{2}m(\dot{r}^2 + r^2\dot{\theta}^2), \quad (3.13)$$

where the last expression comes from Eq. (3.4). The potential energy is given by

$$U = - \int_{\infty}^r \mathbf{F} \cdot d\mathbf{l},$$

where $d\mathbf{l} = \hat{\mathbf{r}}dr$. Therefore,

$$U = - \int_{\infty}^r \frac{K}{r^2} dr = \frac{K}{r}. \quad (3.14)$$

Finally, then, the total energy is

$$\begin{aligned} E &= \frac{1}{2}m\dot{r}^2 + \frac{1}{2}mr^2\dot{\theta}^2 + \frac{K}{r} \\ &= \frac{1}{2}m\dot{r}^2 + \frac{J^2}{2mr^2} + \frac{K}{r}, \end{aligned}$$

where the last expression was obtained by substituting Eq. (3.9).

Since E is a constant of the motion, a convenient θ can be chosen, such as $\theta = 0$. When $\theta = 0$, the time derivative of the radius is also zero; $\dot{r} = 0$. (This can be seen by differentiating Eq. (3.11) with respect to time, and setting $\theta = 0$.) By making these substitutions, and substituting Eq. (3.10) for $\frac{1}{r}$, the expression for total energy can be rewritten as

$$\frac{2E}{m} = \frac{J^2 C^2}{m^2} - \frac{K^2}{J^2}. \quad (3.15)$$

Furthermore, the constant C can be determined from Eq. (3.12). So now f can be determined in terms of the energy of the particle and the charge on the contaminant. Rewriting Eq. (3.15), and making the substitution for C ,

$$f = +\sqrt{1 + \frac{2EJ^2}{mK^2}}, \quad (3.16)$$

where the positive branch of the square root must be taken since $f > 0$ by definition.

In the bulk of the plasma, the potential energy of the particle with respect to the contaminant is zero since $r = \infty$. It is assumed that the particle does have some velocity associated with it as it enters the regions where the force from the contaminant begins to influence its motion. Therefore, the particle has an initial kinetic energy which must be positive, and since total energy is conserved, E must be positive at all radii. This means that the eccentricity of the orbit of the particle about the contaminant must be greater than one. It follows then that the particle sweeps out a hyperbolic trajectory as it passes the contaminant.

3.1.4 Positive Charges

For particles with a positive charge, $q = +e$, and $K < 0$. The hyperbolic path and its geometrical parts are depicted in Fig. 3.3. Note that the particle passes closest to the contaminant when $\theta = 0$. The radius of this distance is given by Eq. (3.11) as,

$$r = \frac{fd}{1+f}.$$

This expression can be written in terms of the angular momentum and the total energy of the particle. Using equations (3.12) and (3.16) and the fact that $d = \frac{1}{C}$, a particle with a given J^2 and E will pass closest to the contaminant at a radius of

$$r = \frac{-\frac{J^2}{KM_+}}{1 + \sqrt{1 + \frac{2EJ^2}{M_+K^2}}}.$$

Rewriting this equation, it can be shown that for a particle to reach a radius of at least r , the total energy and angular momentum must satisfy

$$\frac{J^2}{K^2 M_+^2 r^2} (J^2 + 2M_+ r K - 2M_+ r^2 E) \leq 0.$$

One solution to this inequality is $J = 0$, which is the lower limit for the angular momentum. The upper limit on the square of the angular momentum of the particle is found from the other solution (the term in parenthesis) to this inequality, namely:

$$J^2 \leq 2M_+ r^2 \left(E - \frac{K}{r} \right). \quad (3.17)$$

Note that in Eq. (3.17), E is positive, but K is negative, therefore, J^2 is positive as it must be. Furthermore, all values of E are allowed.

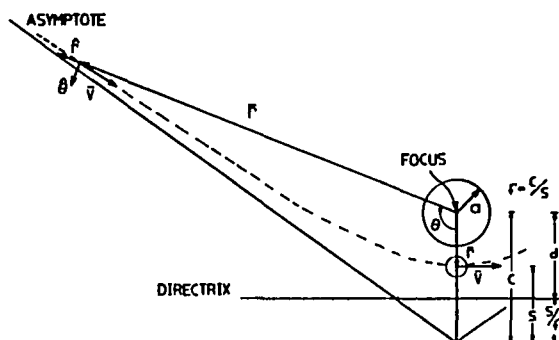


Fig. 3.3 The hyperbolic trajectory of a positive charge under the attractive influence of the contaminant. The particle passes closest to the contaminant when θ goes to zero. When this distance is equal to a , the contaminant radius, the particle is absorbed by the contaminant.

Therefore, the flux of particles to the contaminant can be calculated as follows:

$$\Gamma_+(r) = \int \int \int f_M(u, w) u w d w d \alpha d u,$$

where f_M is the Maxwellian distribution function, u is the radial velocity component, w is the angular component of velocity, and α is the azimuthal angle in velocity space as defined in Fig. 2.2. In terms of the time derivative notation used

to this point, $u = \dot{r}$ and $w = r\dot{\theta}$ as in Eq. (3.4). Therefore, the angular momentum can be written as $J = M_+wr$, and the total energy can be written as

$$\begin{aligned} E &= \frac{1}{2}M_+(u^2 + w^2) + U \\ &= \frac{1}{2}M_+ \left(u^2 + \frac{J^2}{M_+^2 r^2} \right) + \frac{K}{r}. \end{aligned}$$

So the integration can be done in terms of E and J^2 instead of u and w . The Maxwellian distribution function is given by

$$f_M(E) = \frac{N_+}{\pi^{\frac{3}{2}} v_t^3} e^{-E/kT_+},$$

where v_t is the thermal velocity,

$$v_t = \sqrt{\frac{2kT_+}{M_+}}.$$

Therefore, after making the change in integration variables, substituting the Maxwellian function, and after carrying out the integration in α from 0 to 2π , the flux is given by (similar to Eq. (2.17))

$$\Gamma_+(r) = \frac{N_+}{\pi^{\frac{1}{2}} v_t^3 M_+^3 r^2} \int_E \int_{J^2} e^{-E/kT_+} dJ^2 dE. \quad (3.18)$$

In this integration, all values of E are allowed, but for particles to reach a radius r , J^2 is limited as in Eq. (3.17). Therefore, the integration, including the limits becomes

$$\Gamma_+(r) = \frac{N_+}{\pi^{\frac{1}{2}} v_t^3 M_+^3 r^2} \int_0^\infty \int_0^{2M_+r^2(E-K/r)} e^{-E/kT_+} dJ^2 dE.$$

This integration is easily performed, and the result is

$$\Gamma_+(r) = \frac{N_+}{4} \sqrt{\frac{8kT_+}{\pi M_+}} \left(1 - \frac{K}{rkT_+} \right). \quad (3.19)$$

3.1.5 Negative Charges

The flux of negative charges to the contaminant can be computed in a similar manner. It is only necessary to determine the limits of integration for Eq. (3.18). Particles with total energy larger than the potential energy necessary to overcome the repulsive force of the contaminant will collide with the contaminant. That is, $E \geq \frac{K}{r}$, where K is now positive ($q = -e$). Furthermore, the limits on J^2 are determined by requiring the radial kinetic energy to be positive. This can be expressed as

$$J^2 \leq 2m_e r^2 \left(E - \frac{K}{r} \right).$$

For the particle to collide with the contaminant, this condition must be met at $r = a$. Therefore, inserting these limits into Eq. (3.18), the result is

$$\Gamma_e(r) = \frac{N_e}{\pi^{\frac{1}{2}} v_t^3 m_e^3 r^2} \int_{K/r}^{\infty} \int_0^{2m_e r^2 (E - K/r)} e^{-E/kT_e} dJ^2 dE.$$

Finally, the flux of negatively charged particles to the contaminant is found by carrying out this simple integration, namely

$$\Gamma_e(r) = \frac{N_e}{4} \sqrt{\frac{8kT_e}{\pi m_e}} e^{-K/rkT_e}. \quad (3.20)$$

Both Eq. (3.19) and Eq. (3.20) give the flux per unit area of both species of charged particles. The potential that develops on the surface of the contaminant regulates these fluxes in such a way that the total flux of positive charge to the surface is equal to the total flux of negative charge to the surface. Therefore,

$$4\pi a^2 \Gamma_+(a) = 4\pi a^2 \Gamma_e(a).$$

Note, however, that K is negative in Eq. (3.19), but it is positive in Eq. (3.20). This apparent discrepancy can be removed by using the definition of K from Eq. (3.1), and then the value of the charge on the contaminant Q can be determined. Rewriting equations (3.19) and (3.20) in terms of Q , and equating the two equations, yields

$$1 - \frac{Qe}{4\pi\epsilon_0 akT_+} = \sqrt{\frac{T_e}{T_+} \frac{M_+}{m_e}} e^{Qe/(4\pi\epsilon_0 akT_e)}. \quad (3.21)$$

In this equation, the number densities of the two charged species have cancelled out since they are equal.

3.2 RESULTS

The charge on the contaminant can be easily found from Eq. (3.21). From a knowledge of Q , the potential at the surface of the contaminant can be known, the flux of particles to the contaminant can be known, and the electric field at the surface of the contaminant can be known. The results of these calculations will be presented here. The voltage characteristics will be discussed, followed by the flux characteristics. Finally, the results of the charge and electric field calculations will be discussed. These are the results that are necessary in a typical simulation code that deterministically simulates the effects of charged contaminants in the plasma.

3.2.1 Voltage Characteristics

The potential that the contaminant develops can be found from the charge by Eq. (3.14) for the potential energy. In terms of the voltage on the surface of the contaminant, the potential energy is $U = qV(a)$ which by Eq. (3.14) and Eq. (3.1),

$$V(a) = \frac{Q}{4\pi\epsilon_0 a}. \quad (3.22)$$

Futhermore, if the voltage is normalized to the positive ion temperature, as follows

$$y = -\frac{eV(a)}{kT_+}, \quad (3.23)$$

and a parameter β is defined as $\beta = \frac{T_+}{T_e}$, then Eq. (3.21) becomes

$$1 + y = \sqrt{\frac{M_+}{\beta m_e}} e^{-\beta y}. \quad (3.24)$$

This equation can be solved for the normalized potential, which now is only a function of the ratio of positive ion energy to electron energy. There is also a dependence on the mass of the positive ions. This is simply a linear dependence on the square root of the mass. Therefore, for simplicity, all calculations were done

assuming singly ionized argon atoms, $M_+ = 39.44m_p$, where m_p is the rest mass of a proton, and is 1,836 times the mass of the electron.

The dependence of y on the ratio of energies is shown in Fig. 3.4. In this figure, the base ten logarithm of y is plotted against the base ten logarithm of β . The range of β shown is applicable to most plasma etching conditions. Over this range, the relationship between the log of y and the log of β is very nearly linear. In fact, a least squares linear fit is given by the relationship

$$\log y = -0.8527 \log \beta + 0.6638, \quad (3.25)$$

which has a correlation of 99.99%. Using the definition of y in Eq. (3.23), the voltage $V(a)$ is then dependent on the ion and electron energies as follows,

$$V(a) = -4.61T_+^{0.15}T_e^{0.85}, \quad (3.26)$$

where the temperatures are given in electron volts. Note that for a typical ion energy of 0.0258 eV, the contaminant potential is roughly twice the electron energy. This is a useful rule of thumb to estimate the contaminant voltage. It is very important to notice that this result is independent of the size of the contaminant.

3.2.2 Flux Characteristics

Another result that is independent of the size of the contaminant is, quite expectedly, the flux per unit area of particles reaching the contaminant. Either Eq. (3.19) or Eq. (3.20) can be used to determine this flux, since by Eq. (3.21) they should yield the same result. Therefore, for simplicity, Eq. (3.19) will be used. This equation can be written in terms of the contaminant surface potential $V(a)$ by using equations (3.1) and (3.22). The result is,

$$\Gamma_+(a) = \frac{N_+}{4} \sqrt{\frac{8kT_+}{\pi M_+}} \left(1 - \frac{eV(a)}{kT_+} \right).$$

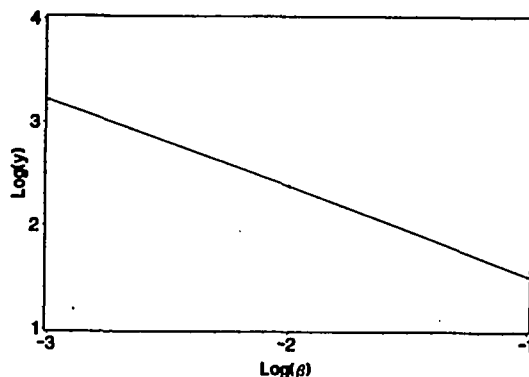


Fig. 3.4 A plot of the normalized contaminant voltage as a function of β . The voltage is independent of the contaminant size.

Furthermore, the result of Eq. (3.26) indicates that the flux is only dependent on the energies of the ions and electrons. This dependency is given by the following relation,

$$\Gamma_+(a) = 6.22 \times 10^4 N_+ T_+^{\frac{1}{2}} (1 + 4.61\beta^{-0.85}).$$

The plot of the flux density for a typical case of $T_+ = 0.0258eV$, and $N_+ = 10^{10}cm^{-3}$ is shown in Fig. 3.5. The flux density has a magnitude of about 10^{16} ions per second per square cm . For a contaminant with a radius of $1\mu m$, the total number of particles impinging on its surface per second is approximately 10^{10} for an electron energy of $4eV$.

Furthermore, if the flux density of particles to the contaminant is normalized to the flux density of positive ions in the bulk of the plasma ($r = \infty$), a normalized flux density γ that is only dependent on β can be defined as follows:

$$\gamma = \frac{\Gamma(a)}{\Gamma(\infty)},$$

where $\Gamma(\infty)$ is given by Eq. (3.19) evaluated at $r = \infty$, and is the flux density of particles in the bulk of the plasma. Note that $y(\infty) = 0$. Consequently,

$$\gamma = 1 + y.$$

Since the normalized voltage is typically much larger than one, it follows that $\gamma \approx y$. Therefore, the characteristic for the normalized voltage shown in Fig. 3.4 is also the characteristic for the normalized flux density.

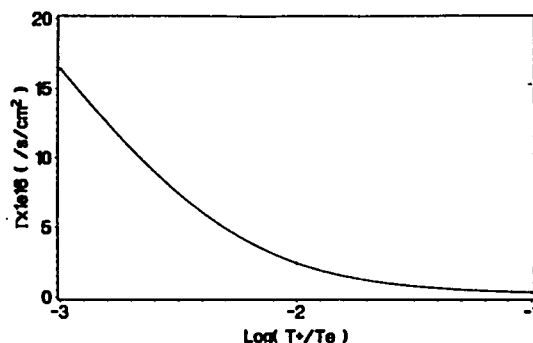


Fig. 3.5 The flux density of one species of charged particles to the surface of the contaminant. The flux density of positive charges is equal to the flux density of negative charges. The total flux density is twice the value given by these curves. $N_+ = 10^{10} \text{ cm}^{-3}$, $T_+ = 0.0258 \text{ eV}$.

3.2.3 Charge Characteristics

The charge on the contaminant is found directly from the surface potential by Eq. (3.22). Therefore, there is a dependence not only on particle energies, but also contaminant size. This seems reasonable since the larger the contaminant, the more surface area there is available for charged particles to cover, therefore a larger charge develops. This phenomenon is demonstrated in Fig. 3.6., where the base ten logarithm of Q is plotted against the base ten logarithm of β . Since Q is linearly dependent on V , the curves are linear with β as a result of the linearity of V mentioned above. Therefore, the charge can be approximated by

$$Q = -5.13 \times 10^{-12} a T_+^{0.15} T_e^{0.85},$$

with a given in cm , and the electron and ion temperatures in electron volts. For example, with 0.0258 eV positive ions, and 4 eV electrons, a $1 \mu m$ contaminant will develop a charge of about -10^{-15} Coulombs, or about 6000 electrons.

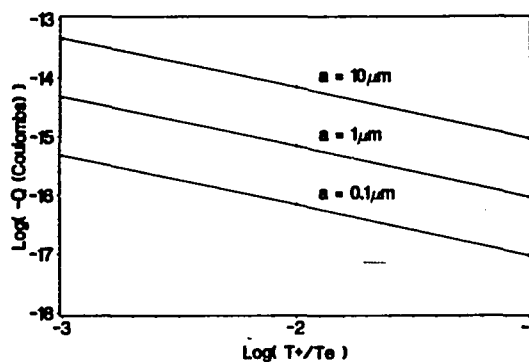


Fig. 3.6 The dependence of the contaminant charge on contaminant size and electron energy. $T_+ = 0.0258 \text{ eV}$.

3.2.4 Electric Field Characteristics

The behavior of the electric field is similar to that of the contaminant charge. The field being discussed here is the field at the surface of the contaminant. In terms of the force exerted by the contaminant on the charge (Eq. (3.1)), the electric field is simply $E = \frac{F}{e}$. Evaluating this expression at $r = a$, it is clear that the electric field is simply related to the surface potential $V(a)$ as $E = \frac{V(a)}{a}$. The curves of the electric field with respect to β are shown in Fig. 3.7. The electric field is on the order of 10^4 to 10^6 volts per centimeter.

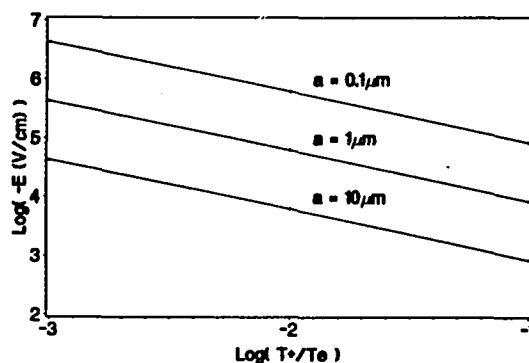


Fig. 3.7 The dependence of the surface electric field on contaminant size and electron energy. $T_+ = 0.0258 \text{ eV}$.

3.3 SUMMARY

In this chapter, it has been shown that for contaminants with radii much smaller than the Debye length, a central force analysis using the Coulomb force is useful. The trajectories of the particles around the contaminant are hyperbolas. The main result of this analysis is the surface potential of the contaminant, for from this quantity, values for the particulate flux density, contaminative charge, and surface electric field can be computed. For typical plasma parameters, the surface potential is roughly twice that of the electron energy.

CHAPTER 4

CONCLUSIONS

Two models for different regions of contaminant size have been developed to describe the electrostatic environment in the vicinity of the contaminant. The Poisson model is useful for contaminants with radii larger than a_{crit} which is on the order of the Debye length. The Coulomb model is useful for contaminants with radii less than a_{crit} .

4.1 POISSON MODEL SUMMARY

The Poisson model requires the integration of Poisson's equation. The number density distribution of each charged species is developed by considering the limits of integration in energy and angular momentum. These limits are imposed by the conservation of energy. The negative charges are assumed to have Maxwellian energy distributions, whereas the positive charges are monoenergetic. The model also requires a knowledge of the flux density of positive ions to the surface of the contaminant. This flux density is the same as the sum of the flux density of negative ions and electrons.

The solution of Poisson's equation requires the use of normalized equations which simplify the problem and define the necessary boundary conditions and constraints. One of the constraints that emerges from the solution is a minimum contaminant radius for which the equations hold. This radius is called a_{crit} , since it is the critical radius that separates the Poisson model region from the Coulomb model region. This critical radius is typically smaller than the Debye length.

4.2 COULOMB MODEL SUMMARY

Since the Poisson model breaks down for contaminants with radii less than the critical radius a_{crit} , it seems reasonable that the number density distribution

no longer plays a significant role in the electrostatics of the contaminant. The fact that the critical radius is less than the Debye length of the Plasma, makes it seem even more plausible that it is only necessary to consider the Coulomb force between the contaminant and the particle. This is the basis of the Coulomb model.

Considering only the Coulomb force makes it relatively simple to determine the flux densities of both the positive and negative charges to the contaminant. In a manner similar to the Poisson model, the limits of integration for flux density determination are determined by the conservation of energy. In this model, however, the positive ions can readily be treated as having a Maxwellian energy distribution, as opposed to being monoenergetic. Once found, the flux densities of the positive and negative charges can be equated. These flux densities are only dependent on the contaminant voltage, positive ion energy, and electron energy. Therefore, the voltage can be found as a function of the particulate energies.

4.3 COMPARISON OF THE TWO MODELS

Both models require some degree of numerical computation. However, the Poisson model is much more involved, requiring the numerical integration of Poisson's equation as well as solutions of several nonlinear equations. The Coulomb model only requires the solution of one nonlinear equation. The most important difference between the two models is their range of applicability. The Poisson model is used to investigate the effects of contaminants with radii on the order of or larger than the Debye length. On the other hand, the Coulomb model is used to investigate the effects of contaminants considerably smaller than the Debye length.

Despite these obvious differences, the results of the calculations with the two models turn out to be surprisingly similar. Both models predict contaminant voltages on the order of the electron energy. The larger contaminants (Poisson model) develop voltages that are weakly dependent on their size. Similarly, the voltages on the smaller contaminants are completely independent of size. Furthermore, the magnitudes of the charges predicted by the two models are roughly of the same order of magnitude, being in the range of -10^{-12} to -10^{-16} Coulombs.

The magnitudes of the flux densities are also comparable. On the other hand, the magnitudes of the electric fields predicted by the Coulomb model are one to three orders of magnitude larger than the electric fields predicted by the Poisson model. This is attributable to the one to three order of magnitude difference in the contaminant sizes, since the voltages are approximately the same.

The characteristics of the electrostatic environment show the same trends between the two models. For example, in both models, the voltages, charges, fluxes, and electric fields all tend to decrease with decreasing electron energy (increasing β). Furthermore, the contaminant charge increases with contaminant size. Additionally, the electric field decreases as the contaminant size increases.

4.4 SUGGESTIONS FOR FURTHER INVESTIGATION

The fact that the Poisson model predicts a voltage that is almost independent of contaminant size, and the Coulomb model predicts a voltage that is independent of size suggests that a transitional region exists between the two models. This region might be modeled by the Debye-shielded Coulomb potential similar to Eq. (1.1). Such a description incorporates some elements of both the Poisson and Coulomb models. The Debye shielding would be a consequence of the number density distributions of the charged particles.

Furthermore, investigation might be made into the physical reasons why Poisson's equation breaks down at a_{crit} . One possible explanation for this might be that the critical radius is small enough that the particular effective potential energy curve for monoenergetic positive ions of angular momentum $J_0 = E_0$ does not intersect the contaminant radius. This would mean that no particles would be absorbed by the contaminant. This conclusion does not correspond to intuition, and so it might be expected that Poisson's equation does not accurately describe this situation.

Finally, much work needs to be done in the application of models like these to plasma simulation codes. These models can assist the simulation codes to determine the effects of many contaminants in the plasma. Questions regarding how the contaminants affect the plasma parameters, and where the contaminants congregate in the plasma could be answered. Perhaps some of the phenomena observed by Selwyn and others could be explained. Additionally, the presence of contaminants in the plasma provides a source of volume recombination for the charged particles. This volume recombination might be expected to significantly affect the plasma sheath potential, and should be investigated. Ultimately, clues as to the origins of these contaminants might be gleaned and used to assist in the prevention and removal of contamination in plasma environments.

APPENDIX A

PROGRAM LISTING FOR COMPUTATIONS
WITH THE POISSON MODEL

```

PROGRAM MENU
10  WRITE (6, '(15X,A)') ' ***** MENU
C ***** '
  WRITE (6, '(15X,A)') '          1 -> START EXECUTION
C
  WRITE (6, '(15X,A)') '          2 -> EXECUTE A
C SINGLE CASE
  WRITE (6, '(15X,A)') '          3 -> RESTART AN
C INCOMPLETE EXECUTION
  WRITE (6, '(15X,A)') '          4 -> STOP EXECUTION
C
20  READ (5,*) M

      IF (M.EQ.1) THEN

          OPEN (UNIT = 40, FILE = '[.DATA]PARTICLE.DAT',
C STATUS = 'NEW')

          ISTART = 1.0
          KSTART = 1.0
          JSTART = 1.0
          CALL PARTICLE(ISTART,KSTART,JSTART)

      ELSE IF (M.EQ.2) THEN
          CALL TEST

      ELSE IF (M.EQ.3) THEN

          OPEN (UNIT = 40, FILE =
C '[.DATA]PARTICLE_.DAT', STATUS = 'NEW')

          WRITE (6,*) 'ENTER THE NUMBER OF THE CASE YOU
C WANT TO START WITH:'
          READ (5,*) ICASE

          ISTART = INT(MOD(ICASE,90)/30) + 1
          KSTART = INT(MOD(MOD(ICASE,90),30)/10) + 1
          JSTART = MOD(ICASE,10)

          CALL PARTICLE(ISTART,KSTART,JSTART)

```

```
ELSE IF (M.EQ.4) THEN
  STOP
```

```
ELSE
  WRITE (6,*) ' INVALID CHOICE'
  GOTO 20
ENDIF
```

```
GOTO 10
END
```

```
*****
SUBROUTINE TEST
```

```
IMPLICIT DOUBLE PRECISION (A-H,L-Z)
DOUBLE PRECISION R(7501), V(7501), DVDR(2,7501),
C XOUT(7501), YOUT(7501), DYOUT(10,7501)
CHARACTER ANS
```

```
COMMON /ERRORS/ ICALL, IERREPORT, IERROR
COMMON /PHYSICS/ A, EO, LDEBYE, M_, MI, N_, NE,
C NI, NUM_ELEC, Q, T_, TE, VA
COMMON /PARAMETERS/ ALPHA, BETA1, BETA, IDIR,
C LAMBDA
COMMON /RESULTS/ XOUT, YOUT, DYOUT, KNEXT
COMMON /MISC/ RB,VB,RC,VC
```

```
OPEN (UNIT = 41, FILE = '[.DATA]SINGLE.DAT',
C STATUS = 'NEW')
OPEN (UNIT = 43, FILE = '[.DATA]CASE.DAT', STATUS
C = 'NEW')
OPEN (UNIT = 44, FILE = '[.DATA]VOLT.DAT', STATUS
C = 'NEW')
OPEN (UNIT = 36, FILE = '[.DATA]ERROR.OUT', STATUS
C = 'NEW')
```

```
IERREPORT = 1
```

```
WRITE (41,13) 'XO', 'NI', 'ALPHA', 'TE', 'A
C MIN', 'VA', 'NUM ELEC', 'LAMBDA', 'RB', 'VB', 'RC', 'VC'
```

```
WRITE (6,*) 'ENTER THE VALUES FOR
C M_,MI,NE,NI,EO,T_,TE'
READ (5,*) M_,MI,NE,NI,EO,T_,TE
WRITE (6,*) 'ENTER A 1 IF YOU WANT TO FIND XO MAX'
WRITE (6,*) 'ENTER A 0 IF YOU WANT TO USE AN
C ARBITRARY XO'
```

```

5      READ (5,*) ICONT
      IF (ICONT.NE.0.AND.ICONT.NE.1) THEN
          WRITE (6,*) 'INVALID RESPONSE'
          GOTO 5
      ENDIF
      IF (ICONT.EQ.0) THEN
C TRY: '
          READ (5,*) X0
      ENDIF

      N_ = NI - NE
      A  = 0.1

      CALL POTENTIAL(X0,XA,ICONT)

      IF (IERROR.EQ.-3.OR.IERROR.EQ.-4) THEN
          WRITE (40,11) X0,NI,ALPHA,TE,XA
          WRITE (6,11) X0,NI,ALPHA,TE,XA
      ENDIF
      IF (IERROR.EQ.-3) THEN
          IERROR = 0
          RETURN
      ENDIF
      WRITE (6,*) 'DO YOU WANT SCREEN OUTPUT (S), FILE
C OUTPUT (F), OR BOTH
C (B)'
7      READ (5,'(A)') ANS
      IF (ANS.EQ.'B'.OR.ANS.EQ.'S') THEN
          WRITE (6,*) 'KNEXT = ', KNEXT
          WRITE (6,*) 'ENTER THE STEP RATE FOR SCREEN
C OUTPUT:'
          READ (5,*) KSTEP
          DO I = 1, KNEXT, KSTEP
              WRITE (6,12) XOUT(I), YOUT(I),
C XOUT(I)**2-1, (DYOUT(J,I), J = 1,2)
              ENDDO
              WRITE (6,12) XOUT(KNEXT), YOUT(KNEXT),
C XOUT(KNEXT)**2-1, (DYOUT(J,KNEXT), J=1,2)
          ENDIF
          IF (ANS.EQ.'B'.OR.ANS.EQ.'F') THEN
              DO I = 1, KNEXT
                  WRITE (43,12) XOUT(I), YOUT(I),
C XOUT(I)**2-1, (DYOUT(J,I), J = 1,2)

              ENDDO
          ENDIF
      IF (ANS.NE.'S'.AND.ANS.NE.'F'.AND.ANS.NE.'B') THEN

```

```

        WRITE (6,*) 'INVALID RESPONSE'
        GOTO 7
    ENDIF
    IF (IERROR.EQ.-4) THEN
        IERROR = 0
        RETURN
    ENDIF
    CALL PHYSICS_TEST(R,V,DVDR,ANS,KSTEP)
    WRITE (6,13) 'XO','NI','ALPHA','TE','A
C MIN','VA','NUM ELEC','LAMBDA','RB','VB','RC','VC'
    WRITE (6,10) XO, NI, ALPHA, TE, A*1.OE4, VA,
C NUM_ELEC, LAMBDA, RB, VB, RC, VC
    WRITE (41,10) XO, NI, ALPHA, TE, A*1.OE4, VA,
C NUM_ELEC, LAMBDA, RB, VB, RC, VC
10    FORMAT (1X, F10.5, E10.2, F6.2, F6.1, 2F13.6,
C E12.3, E15.6, 4F10.3)
11    FORMAT (1X,F10.5,E10.2,F6.2,F6.1,F13.6)
12    FORMAT (1X,F7.3,4F12.4)
13    FORMAT (1X,A10,A10,A6,A6,2A13,A12,A15,4A10)
    RETURN
    END

```

```

*****
SUBROUTINE PARTICLE(ISTART,KSTART,JSTART)

```

```

    IMPLICIT DOUBLE PRECISION (A-H,L-Z)
    DOUBLE PRECISION T(10),ND(3)

```

```

    COMMON /ERRORS/ ICALL, IERREPORT, IERROR
    COMMON /PHYSICS/ A, EO, LDEBYE, M_, MI, N_, NE,
C NI, NUM_ELEC, Q, T_, TE, VA
    COMMON /PARAMETERS/ ALPHA, BETA1, BETA, IDIR,
C LAMBDA
    COMMON /MISC/ RB,VB,RC,VC

```

```

    DATA ND/1.0D9,1.0D10,1.0D11/
    DATA T/0.2,0.4,0.6,0.8,1.0,2.0,4.0,6.0,8.0,10.0/

```

```

    WRITE (40,12) 'CASE','XO','NI','ALPHA','TE','A
C MIN','VA','NUM ELEC','LAMBDA','RB','VB','RC','VC'
    WRITE (6,12) 'CASE','XO','NI','ALPHA','TE','A
C MIN','VA','NUM ELEC','LAMBDA','RB','VB','RC','VC'

```

```

    IERREPORT = 0

```

```

    EO = 0.0258
    T_ = 0.0258
    MI = 39.44

```

```

M_ = 39.44

ICASE = 30*(ISTART-1)+10*(KSTART-1)+JSTART-1
DO I = ISTART, 3
  NI = ND(I)
  DO K = KSTART, 3
    NE = 10.0**K * NI/1000.
    N_ = NI - NE
    DO J = JSTART, 10
      ICASE = ICASE + 1
      TE = T(J)
      OPEN (UNIT=36,
C FILE='[.DATA]ERROR.OUT', STATUS='NEW')
      A = 0.1
      CALL POTENTIAL(XO, XA, 1)
      IF (IERROR.EQ.-3.OR.IERROR.EQ.-4) THEN
        WRITE (40,11) ICASE, XO, NI,
C ALPHA, TE, XA
        IERROR = 0
        GOTO 8
      ENDIF
      WRITE (6,10) ICASE, XO, NI, ALPHA, TE, A*1.OE4,
C VA, NUM_ELEC, LAMBDA, RB, VB, RC, VC
      WRITE (40,10) ICASE, XO, NI, ALPHA, TE, A*1.OE4,
C VA, NUM_ELEC, LAMBDA, RB, VB, RC, VC
8      CLOSE (36)
      ENDDO
    ENDDO
  ENDDO
ENDDO

10  FORMAT (1X, I4, F10.5, E10.2, F6.2, F6.1, 2F13.6,
C E12.3, E15.6, 4F10.3)
11  FORMAT (1X, I4, F10.5, E10.2, F6.2, F6.1, F13.6)
12  FORMAT (1X, A4, A10, A10, A6, A6, 2A13, A12, A15, 4A10)

RETURN
END

```

```

*****
SUBROUTINE POTENTIAL(XO, XA, ICONT)

```

```

*****
**** VARIABLES:
**** IERREPORT: DETERMINES THE VERBOSITY OF
**** ERROR RECORDING
**** 0 -> MINIMUM REPORTING
**** 1 -> VERBOSE REPORTING
**** SCALE: THIS FACTOR SCALES THE SIZE OF THE

```

```

**** INTEGRATION
**** INTERVAL
**** TOL: AN UPPER BOUND ON ALLOWABLE
**** INTEGRATION ERROR
**** H1: INITIAL STEPSIZE IN THE INTEGRATION
**** HMIN: MINIMUM STEPSIZE IN THE INTEGRATION
**** ACCEPT: A GENERAL VARIABLE FOR DETERMINING
**** THE ACCEPTABILITY OF VARIOUS RESULTS ****
IDIR: SPECIFIES THE DIRECTION OF THE
**** INTEGRATION
**** -1 -> IN DIRECTION OF
**** DECREASING X
**** 1 -> IN DIRECTION OF
**** INCREASING X
**** MI: ATOMIC MASS OF POSITIVE IONS (A.M.U.)
**** M_: ATOMIC MASS OF NEGATIVE IONS (A.M.U.)
**** NE: NUMBER DENSITY OF ELECTRONS (PER CUBIC
**** CM)
**** NI: NUMBER DENSITY OF POSITIVE IONS (PER
**** CUBIC CM)
**** N_: NUMBER DENSITY OF NEGATIVE IONS (PER
**** CUBIC CM)
**** EO: POSITIVE ION ENERGY (EV)
**** T_: NEGATIVE ION ENERGY (EV)
**** TE: ELECTRON ENERGY (EV)
**** LAMBDA: A MATHEMATICAL PARAMETER OF THE
**** DIFFERENTIAL EQUATION.
**** LDEBYE: THE DEBYE LENGTH OF THE PLASMA
**** BETA: RATIO OF POSITIVE ION ENERGY TO
**** ELECTRON ENERGY
**** BETA1: RATIO OF POSITIVE ION ENERGY TO
**** NEGATIVE ION ENERGY
**** ALPHA: RATIO OF ELECTRON DENSITY TO
**** POSITIVE ION DENSITY
**** A: PARTICLE RADIUS IN CM
**** LAMBDA_MIN: THE VALUE OF LAMBDA AT A GIVEN
**** A AND ZERO PARTICLE VOLTAGE. BELOW THIS C VALUE,
**** THE VOLTAGE IS REQUIRED TO BE POSITIVE AND THE
**** THEORY IS INVALID.
**** X0: POINT AT WHICH BOUNDARY CONDITIONS ARE
**** DEFINED
**** XOUT, YOUT, DYOUT: RESULTS OF THE
**** INTEGRATION ARE STORED IN THESE ARRAYS, IDEXED BY J
**** (NUMBER OF STEP) AND I (ORDER OF DERIVATIVE)
**** ICALL: COUNT OF NUMBER OF TIMES
**** DIFFERENTIAL EQUATION IS EVALUATED.
**** KNEXT: NUMBER OF THE NEXT STEP TO BE TAKEN
**** IN THE INTEGRATION

```

```

****          IERROR: ERROR FLAG
****          0 -> NO ERROR
****          1 -> SOLUTION CROSSED
****          X**2-1, SQRT(-1), MAKE LAMBDA SMALLER
****          2 -> SOLUTION TOWARD
****          ORIGIN DIVERGING INCREASE LAMBDA
****          3 -> X=0.0 IN EVALUATION
****          OF DIFF.EQ. VARIABLE NOT PASSED, OR INT. DONE
****          4 -> LAMMDA*X**4=0.0 IN
****          EVAL. OF DIFF.EQ. VARIABLES NOT PASSED, OR VERY
****          SMALL
****          6 -> Y<0.0 IN EVALUATION
****          OF DIFF.EQ.
****          11-> STEPSIZE<HMIN IN
****          INTEGRATION, FIX TOL
****          12-> TOO MANY STEPS IN
****          INTEGRATION INTERVAL
****          10-> STEPSIZE=0.0, FIX TOL
**** SUBROUTINES AND FUNCTIONS:
****          DZREAL: AN IMSL SUBROUTINE THAT FINDS THE
****          REAL ZEROS OF A FUNCTION. INITIAL GUESSES ARE
****          SPECIFIED IN X, ZEROS ARE RETURNED IN XZ WITH THE
****          NUMBER OF ITERATIONS IN INFO.
****          POISSON: EVALUATES POISSON'S EQUATION AND
****          MONITORS FOR CONVERGENCE OF SOLUTION TO ENDPOINTS.
****          DRVTVS: THE SECOND ORDER DIFFERENTIAL
****          EQUATIONS. THIS ALSO MONITORS INTEGRATION
****          CONDITIONS FOR ERRORS.
****          ODEINT: INTEGRATION DRIVER ROUTINE,
****          CONTROLS RUNGE-KUTTA ALGORITHM.
****          RKQC: MONITORS AND ADJUSTS STEPSIZE TO
****          MAINTAIN ERROR TOLERANCE.
****          RKN4: 4TH ORDER RUNGE-KUTTA-NYSTROM
****          ALGORITHM.
****          PHYSICS: CONVERTS THE MATHEMATICAL
****          PARAMETERS TO PHYSICAL PARAMETERS.
****          ERROR_HANDLER: DETERMINES AND CORRECTS
****          ERRORS
*****
****          IMPLICIT DOUBLE PRECISION (A-H,L-Z)
****          DOUBLE PRECISION V(7501),R(7501),DVDR(2,7501)
****          DOUBLE PRECISION XOUT(7501), YOUT(7501),
C DYOUT(10,7501)

****          COMMON /ERRORS/ ICALL, IERREPORT, IERROR
****          COMMON /PHYSICS/ A, EO, LDEBYE, M_, MI, N_, NE,
C NI, NUM_ELEC, Q, T_, TE, VA
****          COMMON /PARAMETERS/ ALPHA, BETA1, BETA, IDIR,

```

```

C LAMBDA
COMMON /RESULTS/ XOUT, YOUT, DYOUT, KNEXT
COMMON /MISC/ RB,VB,RC,VC

EXTERNAL DRVTVS1, DRVTVS2, F, FX0, F1, F2

PARAMETER (ZERO = 0.0, PI = 3.141592654, ACCEPT =
C 0.2)

```

```

**** INITIALIZE CONTROL VARIABLES.

```

```

SCALE      = 0.02
TOL        = 0.1
H1         = 0.01
HMIN       = 0.0001
IDIR       = 1
A          = 0.1
IXO        = 0.0

```

```

**** CALCULATE VARIOUS PHYSICAL PARAMETERS.

```

```

N_         = NI - NE
LDEBYE    = 743.4041 * SQRT(TE/NE)
BETA      = EO / TE
BETA1     = EO / T_
ALPHA     = NE / NI

```

```

*** Find XA for A_MIN.

```

```

XGUESS = SQRT(SQRT(4./PI*MI*1836./BETA) * (ALPHA +
C (1-ALPHA) * SQRT(T_/(TE*1836*M_))))

```

```

CALL DZREAL(F, 1.0E-5, 1.0E-5, 1.0E-5, 0.01, 1,
C 100, XGUESS, XA, INFO)

```

```

YA = XA**2 - 1
VA = -EO * YA
IF (ICONT.EQ.0) THEN
  GOTO 10

```

```

ENDIF

```

```

X1 = 1.5

```

```

CALL DZREAL(F1, 1.0E-8, 1.0E-8, 1.0E-5, 0.01, 1,
C 100, X1, XZ, INFO)

```

```

X1 = 3.0

```

```

CALL DZREAL(F2, 1.0E-8, 1.0E-8, 1.0E-5, 0.01, 1,
C 100, X1, XM, INFO)

```

```

YM = 1.0 - XM**2

```

```

LAMBDA = (XM/2.0-ALPHA*EXP(BETA*YM)-(1-ALPHA)*
C EXP(BETA1*YM))/2.0/XM**4

```

```

XL = XM

```



```

XS = XZ

XO = (XZ + XM) / 2
YO = 1.0 - XO**2
10 LAMBDA = (XO/2.0-ALPHA*EXP(BETA*YO)-(1-ALPHA)*
C      EXP(BETA1*YO))/2.0/XO**4

IF (XA.LE.XO) THEN
  WRITE (36,*) 'XA IS NOT LARGER THAN XO'
  IERROR = -3
  RETURN
ENDIF
IF (ICONT.EQ.0) THEN
  XFINAL = XO + 7500.*SCALE*IDIR
  GOTO 12
ENDIF
XFINAL = XA + 0.01
JSAV   = NINT((XFINAL-XO)/SCALE)+1
XFINAL = XA + 0.02

**** INITIALIZE RESULT ARRAYS, INTEGRATION COUNTERS, AND
**** ERROR FLAG.
IF (JSAV.GT.KNEXT) THEN
  JLAST = JSAV
ELSE
  JLAST = KNEXT
ENDIF
12 DO J = 1, JLAST
  XOUT(J) = 0.0
  YOUT(J) = 0.0
  DO I = 1, 2
    DYOUT(I,J) = 0.0
  ENDDO
ENDDO

IXO   = IXO + 1
ICALL = 0
KNEXT = 0
IERROR = 0

**** DO THE INTEGRATION.
CALL POISSON(XO, XFINAL, H1, HMIN, TOL, SCALE,
C ICONT, DRVTVS1)

IF (IERROR.NE.0.AND.IERROR.NE.1) THEN
  CALL ERROR_HANDLER(XO,XFINAL,TOL,SCALE)
ENDIF
IF (ICONT.EQ.0) THEN

```

```

        GOTO 16
    ENDIF
    IF (XL.EQ.X0.OR.XS.EQ.X0) THEN
        WRITE (36,*) 'IXO = ', IXO
        WRITE (36,*) 'XO = ', X0, ' LAMBDA = ',
C LAMBDA
        WRITE (36,*) 'XL = ', XL, ' XS = ', XS
        WRITE (36,*) 'XM = ', XM, ' XZ = ', XZ
        WRITE (36,*) 'XL = XS'
        IF (IERREPORT.EQ.1) THEN
            WRITE (6,*) 'IXO = ', IXO
            WRITE (6,*) 'XO = ', X0, ' LAMBDA = ',
C LAMBDA
            WRITE (6,*) 'XL = ', XL, ' XS = ', XS
            WRITE (6,*) 'XM = ', XM, ' XZ = ', XZ
            WRITE (6,*) 'XL = XS'
        ENDIF
        IERROR = -4
        RETURN
    ELSE IF (YOUT(JSAV).EQ.ZERO) THEN
        IF (IERREPORT.EQ.1) THEN
            WRITE (6,*) 'XO TOO LARGE'
            WRITE (6,*) 'IXO = ', IXO
            WRITE (6,*) 'XO = ', X0, ' LAMBDA = ',
C LAMBDA
            WRITE (6,*) 'XL = ', XL, ' XS = ', XS
            WRITE (6,*) 'XM = ', XM, ' XZ = ', XZ
        ENDIF
        XL = X0
        X0 = (XS + XL) / 2.0
        WRITE (36,*) 'XO TOO LARGE'
        WRITE (36,*) 'IXO = ', IXO
        WRITE (36,*) 'XO = ', X0, ' LAMBDA = ',
C LAMBDA
        WRITE (36,*) 'XL = ', XL, ' XS = ', XS
        WRITE (36,*) 'XM = ', XM, ' XZ = ', XZ
        GOTO 10
    ELSE IF (YOUT(JSAV)-XOUT(JSAV)**2+1.GT.ACCEPT)
THEN
        IF (IERREPORT.EQ.1) THEN
            WRITE (6,*) 'XO TOO SMALL'
            WRITE (6,*) 'IXO = ', IXO
            WRITE (6,*) 'XO = ', X0, ' LAMBDA = ',
C LAMBDA
            WRITE (6,*) 'XL = ', XL, ' XS = ', XS
            WRITE (6,*) 'XM = ', XM, ' XZ = ', XZ
        ENDIF
        XS = X0

```

```

      XO = (XS + XL) / 2.0
      WRITE (36,*) 'XO TOO SMALL'
      WRITE (36,*) 'IXO = ', IXO
      WRITE (36,*) 'XO = ', XO, ' LAMBDA = ',
C LAMBDA
      WRITE (36,*) 'XL = ', XL, ' XS = ', XS
      WRITE (36,*) 'XM = ', XM, ' XZ = ', XZ
      GOTO 10
    ENDIF
    IF (IERREPORT.EQ.1) THEN
      WRITE (6,'(1X,A,I6,A,F20.10)') ' XA MAX FOUND:
C XOUT(' ,JSAV,') = ', XOUT(JSAV)
      WRITE (6,*) ' XA = ', XA
      WRITE (6,'(1X,A,I4,A)') 'THERE WERE ', IXO, '
C ITERATIONS ON XO'
    ENDIF
    WRITE (36,'(1X,A,I6,A,F20.10)') ' XA MAX FOUND:
C XOUT(' ,JSAV,') = ', XOUT(JSAV)
    WRITE (36,*) ' XA = ', XA
15   WRITE (36,'(1X,A,I4,A)') 'THERE WERE ', IXO, '
C ITERATIONS ON XO'

**** IF ALL THE ABOVE IS SUCCESSFUL:
**** CALCULATE PHYSICAL PARAMETERS FROM MATHEMATICAL
C PARAMETERS.
16   CALL PHYSICS(R,V,DVDR)

      RETURN
      END

```

```

*****
      SUBROUTINE POISSON(XO, XFINAL, H1, HMIN, TOL,
C SCALE, ICONT, DRVTVS)

```

```

**** This program uses a fourth-order Runge-Kutta-Nystrom
**** integrator ODEINT to numerically integrate Poisson's
**** equation describing a particle in a collisionless
**** plasma. The actual form of Poisson's equation is
**** defined in a subroutine DRVTVS which evaluates the
**** second derivative DYDX(2) given values for the first
**** derivative DYDX(1) and the function Y at a known
**** point X. BETA and LAMBDA are physical in Poisson's
**** equation. The error of accuracy in the is regulated
**** by TOL. A guessed first step size H1, and a minimum
**** step size HMIN are reported to ODEINT. ODEINT
**** returns the number of and retried steps NBAD, and
**** the number of succesful steps NOK. Y and are
**** returned with the approximated values at XEND.

```

**** The common variable flags various numerical
 **** conditions. Negative values and values 1 to 10 are
 **** reserved for conditions arising in DRVTVS. Values
 **** 10 larger are reserved for use in ODEINT.

```

      IMPLICIT DOUBLE PRECISION (A-H,L-Z)
      DOUBLE PRECISION DYDX(2), XOUT(7501), YOUT(7501),
C DYOUT(10,7501), TEST(7501)

```

```

      COMMON /ERRORS/ ICALL, IERREPORT, IERROR
      COMMON /PHYSICS/ A, EO, LDEBYE, M_, MI, N_, NE,
C NI, NUM_ELEC, Q, T_, TE, VA
      COMMON /PARAMETERS/ ALPHA, BETA1, BETA, IDIR,
C LAMBDA
      COMMON /RESULTS/ XOUT, YOUT, DYOUT, KNEXT
      COMMON /PARTICLE/ XA

```

```

      PARAMETER (ACCEPT = 0.2, ZERO = 0.0, PI =
C 3.141592654)

```

```

      EXTERNAL DRVTVS, FYA

```

```

      INCREASE = 0

```

**** DETERMINE INITIAL CONDITIONS.

```

      Y          = X0**2.0 - 1.0
      DYDX(1)    = 2.0 * X0
      X          = X0
      XOUT(1)    = X
      YOUT(1)    = Y
      DYOUT(1,1) = DYDX(1)
      CALL DRVTVS(X,Y,DYDX)
      IF (IERROR.GT.0) THEN
        RETURN
      ENDIF
      DYOUT(2,1) = DYDX(2)

```

**** DO LOOP STEPS INTEGRATOR THROUGH SPECIFIED INTERVALS.

```

      DO XEND = X0 + SCALE*IDIR, XFINAL, SCALE*IDIR
        KNEXT = KNEXT + 1
        YSAV = Y
        CALL ODEINT(X, XEND, Y, DYDX, TOL, H1, HMIN,
C NOK, NBAD, DRVTVS)

        IF (IERROR.NE.0.AND.ICONT.EQ.1) THEN
          RETURN
        ELSE IF (IERROR.NE.0.AND.IERROR.NE.1
C .AND.ICONT.EQ.0) THEN

```

```

        RETURN
    ENDIF

    X = XEND

**** STORE RESULTS OF SUCCESSFULL INTEGRATIONS.
    XOUT(KNEXT+1) = X
    YOUT(KNEXT+1) = Y
    DO J = 1, 2
        DYOUT(J,KNEXT+1) = DYDX(J)
    ENDDO
    IF (ICONT.EQ.1) THEN
        GOTO 29
    ENDIF
    IF (IERROR.EQ.1) THEN
        XA = XOUT(KNEXT)
        YA = YOUT(KNEXT)
        CALL DZREAL(FYA, 1.E-5, 1.E-5, 1.E-5, .01,
C 1, 100, YA, YA, INFO)
        WRITE (6,24) 'XA', 'YOUT', 'YA'
        WRITE (6,25) XA, YOUT(KNEXT), YA
        VA = -E0*YA
        KNEXT = KNEXT - 1
        GOTO 30
    ENDIF
24     FORMAT (3A20)
25     FORMAT (3F20.8)
**** CHECK IF THE PARTICLE HAS BEEN REACHED. IF IT HAS,
**** THE INTEGRATION IS DONE. IF NOT, CONTINUE.
        TEST(KNEXT+1) = X - SQRT( SQRT( 4. / PI *
C 1836. * MI / BETA) * (ALPHA * EXP(-BETA * Y) +
C (1-ALPHA) * SQRT( T_ / ( TE * 1836. * M_ ) ) *
C EXP(-BETA1 * Y )))
        IF (TEST(KNEXT+1).GE.ZERO) THEN
            IF (ABS( TEST(KNEXT+1)) .LE. ABS(
C TEST(KNEXT))) THEN
                XA = XOUT(KNEXT+1)
                YA = YOUT(KNEXT+1)
                CALL DZREAL(FYA, 1.E-5, 1.E-5, 1.E-5,
C .01, 1, 100, YA, YA, INFO)
                WRITE (6,24) 'XA', 'YOUT', 'YA'
                WRITE (6,25) XA, YOUT(KNEXT+1), YA
                VA = -E0*YA
                GOTO 30
            ELSE
                XA = XOUT(KNEXT)
                YA = YOUT(KNEXT)
                CALL DZREAL(FYA, 1.E-5, 1.E-5, 1.E-5,

```

```

C .01, 1, 100, YA, YA, INFO)
      WRITE (6,24) 'XA', 'YOUT', 'YA'
      WRITE (6,25) XA, YOUT(KNEXT), YA
      VA = -EO*YA
      KNEXT = KNEXT - 1
      GOTO 30

```

```

      ENDIF
    ENDIF

```

```

29      ENDDO
30      KNEXT = KNEXT + 1
      RETURN
      END

```

```

*****

```

```

      SUBROUTINE DRVTVS1(X,Y,DYDX)

```

```

      IMPLICIT DOUBLE PRECISION (A-H,L-Z)
      DOUBLE PRECISION DYDX(2)

```

```

      COMMON /ERRORS/ ICALL, IERREPORT, IERROR
      COMMON /PARAMETERS/ ALPHA, BETA1, BETA, IDIR,

```

```

C LAMBDA

```

```

      PARAMETER (SMALL = 1E-16)

```

```

      ICALL = ICALL + 1
      U      = 1.0 + Y
      V      = U - X**2.0

```

```

      IF (V.LT.ZERO) THEN

```

```

        IERROR = 1

```

```

        IF (IERREPORT.EQ.1) THEN

```

```

          WRITE (6,*) 'IERROR =', IERROR, ' ICALL

```

```

C =', ICALL

```

```

          WRITE (6,*) 'X =', X, ' Y =', Y

```

```

          WRITE (6,*) 'U =', U, ' V =', V

```

```

        ENDIF

```

```

        WRITE (36,*) 'IERROR =', IERROR, ' ICALL =',

```

```

C ICALL

```

```

        WRITE (36,*) 'X =', X, ' Y =', Y

```

```

        WRITE (36,*) 'U =', U, ' V =', V

```

```

        IF (ABS(V) .LE. SMALL .AND. ICALL .LT. 100

```

```

C .AND. IDIR .GT. 0) THEN

```

```

          WRITE (36,*) 'SETTING V TO 0.0'

```

```

          WRITE (6,*) 'SETTING V TO 0.0'

```

```

          V = 0.0

```

```

          IERROR = 0

```

```

ELSE
  RETURN
ENDIF
ENDIF

```

```

DYDX(2) = (0.5*SQRT(U) - IDIR*0.5*SQRT(V) -
C ALPHA*EXP(-BETA*Y) - (1-ALPHA)*EXP(-BETA1*Y)) /
C (LAMBDA * X**4.0)

```

```

RETURN
END

```

```

*****
SUBROUTINE DRVTVS2(X1,Y,DYDX1)

```

```

*** This subroutine evaluates the second derivative of
*** Poisson's equation where it is expressed as a
*** function of X, Y, and DYDX(1) (the first derivative).
*** The second derivative is named DYDX(2). This
*** subroutine evaluates a normalized Poisson's equation
*** for a particle in a collision-less plasma valid in
*** the region  $0 < X < X_0$ . The form of Poisson's equation
*** requires division by fourth power of X. The IF
*** structure below prevents division by zero. It is
*** reasonable to expect that Y, DYDX(1), and DYDX(2) all
*** approach with X. In fact, that is one of the
*** boundary conditions of the at hand. The structure
*** also flags negative values for Y, and prevents taking
*** the square root of a negative value.

```

```

IMPLICIT DOUBLE PRECISION (A-H,L-Z)
DOUBLE PRECISION DYDX(2), DYDX1(2), I1

```

```

COMMON /ERRORS/ ICALL, IERREPORT, IERROR
COMMON /PARAMETERS/ ALPHA, BETA1, BETA, IDIR,
C LAMBDA

```

```

ICALL = ICALL + 1

```

```

IF (X1.EQ.ZERO) THEN
  IERROR = 3
  DYDX(2) = 0.0
  RETURN
ENDIF

```

```

I1 = ALPHA * BETA / LAMBDA
X = SQRT(I1) / X1
DYDX(1) = (-1)*X1*2/SQRT(I1)* DYDX1(1)

```

```

U      = 1.0 + Y
V      = U - I1/X**2.0
BETA1  = BETA * BETA1

IF (U.LT.ZERO.OR.V.LT.ZERO) THEN
  IERROR = 1
  IF (IERREPORT.EQ.1) THEN
    WRITE (36,*) 'IERROR =', IERROR, ' ICALL
C =', ICALL
    WRITE (36,*) 'X =', X, ' Y =', Y
    WRITE (36,*) 'U =', U, ' V =', V
  ENDIF
  RETURN
ENDIF

DYDX(2) = (0.5 * SQRT(U) - IDIR * 0.5 * SQRT(V)
C - ALPHA * EXP(-BETA * Y) - (1 - ALPHA) *
C EXP(-BETA1 * Y)) / (ALPHA * BETA) - 2 / X * DYDX(1)

DYDX1(2) = X**4/I1*(DYDX(2)+2/X*DYDX(1))

RETURN
END

```

```
*****
```

```
DOUBLE PRECISION FUNCTION F(X)
```

```
IMPLICIT DOUBLE PRECISION (A-H,L-Z)
```

```
PARAMETER (PI = 3.141592654)
```

```
COMMON /PHYSICS/ A, EO, LDEBYE, M_, MI, N_, NE,
C NI, NUM_ELEC, Q, T_, TE, VA
COMMON /PARAMETERS/ ALPHA, BETA1, BETA, IDIR,
C LAMBDA
```

```

F = X - SQRT( SQRT( 4. / PI * 1836. * MI / BETA)
C * (ALPHA * EXP(-BETA * (X**2 - 1) + (1 - ALPHA) *
C SQRT(T_ / (TE * 1836. * M_)) * EXP(-BETA1 *
C (X**2 - 1))))

```

```
RETURN
END
```

```
*****
```

```
DOUBLE PRECISION FUNCTION FX0(X0)
```

```
IMPLICIT DOUBLE PRECISION (A-H,L-Z)
```



```

PARAMETER (PI = 3.141592654)

COMMON /PHYSICS/ A, EO, LDEBYE, M_, MI, N_, NE,
C NI, NUM_ELEC, Q, T_, TE, VA
COMMON /PARAMETERS/ ALPHA, BETA1, BETA, IDIR,
C LAMBDA

FXO = (XO / 2.0 - ALPHA * EXP(-BETA * (XO**2.0 -
C 1.0)) - (1 - ALPHA) * EXP(-BETA1 * (XO**2.0 -
C 1.0))) / (2.0 * XO**4.0)

RETURN
END

```

```

*****
DOUBLE PRECISION FUNCTION FYA(Y)

```

```

IMPLICIT DOUBLE PRECISION (A-H,L-Z)

COMMON /PARTICLE/ X
COMMON /PHYSICS/ A, EO, LDEBYE, M_, MI, N_, NE,
C NI, NUM_ELEC, Q, T_, TE, VA
COMMON /PARAMETERS/ ALPHA, BETA1, BETA, IDIR,
C LAMBDA

PARAMETER (PI = 3.141592654)

FYA = X - SQRT( SQRT( 4. / PI * 1836. * MI / BETA)
C * (ALPHA * EXP(-BETA * Y) + (1 - ALPHA) * SQRT( T_
C / (TE * 1836. * M_) * EXP(-BETA1 * Y)))

RETURN
END

```

```

*****
DOUBLE PRECISION FUNCTION F1(X)

```

```

IMPLICIT DOUBLE PRECISION (A-H,L-Z)
COMMON /PARAMETERS/ ALPHA, BETA1, BETA, IDIR,
C LAMBDA

Y = 1.0 - X**2
F1 = (X / 2.0 - ALPHA * EXP(BETA * Y) - (1 -
C ALPHA) * EXP(BETA1 * Y)) / 2.0 / X**4

RETURN
END

```

```
*****
DOUBLE PRECISION FUNCTION F2(X)
```

```
IMPLICIT DOUBLE PRECISION (A-H,L-Z)
COMMON /PARAMETERS/ ALPHA, BETA1, BETA, IDIR,
C LAMBDA
```

```
Y = 1.0 - X**2
F2 = ALPHA * (BETA * X**2 + 2.) * EXP(BETA * Y)
C + (1 - ALPHA) * (BETA1 * X**2 + 2.) * EXP(BETA1 *
C Y) - 0.75 * X
```

```
RETURN
END
```

```
*****
SUBROUTINE ODEINT(X1, X2, Y, DYDX, EPS, H1, HMIN,
C NOK, NBAD, DRVTVS)
```

```
*** Runge-Kutta driver with adaptive stepsize control.
**** Integrate the two starting values Y and DYDX(1) from
**** X1 to X2 with accuracy EPS. H1 should be set as a
**** guessed first step size, HMIN as the minimum allowed
**** stepsize. On output NOK and NBAD are the number of
**** good and bad (but retried and fixed) steps taken, and
**** Y and DYDX(1) are replaced by values at the end of
**** the integration interval. DRVTVS is the
**** user-supplied subroutine for calculating the value of
**** the second derivative. RKQC is the name of the
**** stepper routine.
```

```
IMPLICIT DOUBLE PRECISION (A-H,O-Z)
DOUBLE PRECISION YSCAL(2), DYDX(2)
COMMON /ERRORS/ ICALL, IERREPORT, IERROR
PARAMETER (MAXSTP=10000,ZERO=0.0,TINY=1.E-30)
EXTERNAL DRVTVS
```

```
X      = X1
H      = SIGN(H1,X2-X1)
NOK    = 0
NBAD   = 0
NSHRNK = 0
```

```
DO NSTP = 1, MAXSTP
```

```
CALL DRVTVS(X,Y,DYDX)
IF (IERROR.GT.0) THEN
```

```

                RETURN
            ENDIF
**** SCALING USED TO MONITOR ACCURACY.
        YSCAL(1) = ABS(Y) + ABS(H*DYDX(1)) + TINY
        YSCAL(2) = ABS(DYDX(1)) + ABS(H*DYDX(2)) +
C TINY

**** MAKE SURE STEP DOES NOT OVERSHOOT END.
        IF ((X+H-X2)*(X+H-X1).GT.ZERO) THEN
            H = X2 - X
        ENDIF

        CALL RKQC(X, Y, DYDX, EPS, YSCAL, H, HDID,
C HNEXT, NSHRNK, DRVTVS)
        IF (IERROR.GT.0) THEN
            RETURN
        ENDIF

        IF (HDID.EQ.H) THEN
            NOK = NOK+1
        ELSE
            NBAD = NBAD+1
        ENDIF

**** CHECK FOR END.
        IF ((X-X2)*(X2-X1).GE.ZERO) THEN
            RETURN
        ENDIF

        IF (ABS(HNEXT).LT.HMIN) THEN
            IERROR = 11
            IF (IERREPORT.EQ.1) THEN
                WRITE (36,*) 'IERROR =', IERROR, '
C ICALL =', ICALL
                WRITE (36,*) 'NOK =', NOK, ' NBAD =',
C NBAD
                WRITE (36,*) 'HNEXT =', HNEXT, ' HMIN
C =', HMIN
                WRITE (36,*) 'NSTP =', NSTP
            ENDIF
            RETURN
        ENDIF

        H = HNEXT

    ENDDO

    IERROR = 12

```

```

      IF (IERREPORT.EQ.1) THEN
        WRITE (36,*) 'IERROR =', IERROR, ' ICALL =',
C ICALL
        WRITE (36,*) 'NOK =', NOK, ' NBAD =', NBAD
        WRITE (36,*) 'NSTP =', NSTP, ' MAXSTP =',
C MAXSTP
      ENDIF

      RETURN
      END

```

```

*****
      SUBROUTINE RKQC(X, Y, DYDX, EPS, YSCAL, HTRY,
C HDID, HNEXT, NSHRNK, DRVTVS)

```

```

*** Fifth-order Runge-Kutta step with monitoring of local
**** truncation error to ensure accuracy and adjust
**** stepsize. Input are the variable Y and its first and
**** second derivatives DYDX(1) and DYDX(2) at the
**** starting value of the variable X. Also input are the
**** stepsize to be attempted HTRY, the required accuracy
**** EPS, and the vector YSCAL against which the error is
**** scaled. On output, Y and X are replaced by their new
**** values, HDID is the stepsize which was actually
**** accomplished, and HNEXT is the estimated next
**** stepsize. DRVTVS is the user-supplied subroutine
**** that computes the second derivative.

```

```

      IMPLICIT DOUBLE PRECISION (A-H,O-Z)
      DOUBLE PRECISION DYDX(2), YSCAL(2), DYSAV(2)
      COMMON /ERRORS/ ICALL, IERREPORT, IERROR
      PARAMETER (PGROW=-0.20, PSHRNK=-0.25, FCOR=1./15.,
C ONE=1., SAFETY=0.9, ERRCON=6.E-4, ZERO = 0.0)
      EXTERNAL DRVTVS

```

```

**** SAVE INITIAL VALUES.
      XSAV = X
      YSAV = Y
      DO I = 1, 2
        DYSAV(I) = DYDX(I)
      ENDDO

```

```

      H = HTRY
1      HH = H / 2.0

```

```

**** TAKE TWO HALF-STEPS.
      CALL RKN4(X, YSAV, DYSAV, HH, YTEMP, DRVTVS)
      IF (IERROR.GT.0) THEN

```

```

        RETURN
    ENDIF

    X = XSAV + HH

    DYDX(1) = DYSAV(1)
    CALL DRVTVS(X, YTEMP, DYDX)
    IF (IERROR.GT.0) THEN
        RETURN
    ENDIF

    CALL RKN4(X, YTEMP, DYDX, HH, Y, DRVTVS)
    IF (IERROR.GT.0) THEN
        RETURN
    ENDIF

    X = XSAV + H

    IF (X.EQ.XSAV) THEN
        IERROR = 10
        IF (IERREPORT.EQ.1) THEN
            WRITE (36,*) 'IERROR =', IERROR, ' ICALL
C =', ICALL
            WRITE (36,*) 'X =', X, ' H =', H
        ENDIF
        RETURN
    ENDIF

**** TAKE THE FULL-SIZE STEP.
    CALL RKN4(XSAV, YSAV, DYSAV, H, YTEMP, DRVTVS)
    IF (IERROR.GT.0) THEN
        RETURN
    ENDIF

**** EVALUATE THE ACCURACY BY SUBTRACTING THE RESULTS OF
**** THE FULL SIZE STEP FROM THE RESULTS OF THE TWO HALF
**** SIZE STEPS.
    ERRMAX = 0.
    YTEMP = Y - YTEMP
    DYTEMP = DYDX(1) - DYSAV(1)
    ERRMAX = MAX(ERRMAX, ABS(YTEMP/YSCAL(1)))
    ERRMAX = MAX(ERRMAX, ABS(DYTEMP/YSCAL(2)))
    ERRMAX = ERRMAX/EPS

**** IF SCALED ERROR IS TOO LARGE, REDUCE THE STEPSIZE AND
**** TRY AGAIN. IF ERROR ACCEPTABLE, STEP SUCCEEDED.
**** DETERMINE NEXT STEP SIZE.

```

```

IF (ERRMAX.GT.ONE) THEN
  H = SAFETY * H * (ERRMAX**PSHRNK)
  IF (IERREPORT.EQ.1) THEN
    NSHRNK = NSHRNK + 1
    WRITE (36,*) 'NSHRNK =', NSHRNK, ' H =',
C H
    ENDIF
    GOTO 1
ELSE
  HDID = H
  IF (ERRMAX.GT.ERRCON) THEN
    HNEXT = SAFETY * H * (ERRMAX**PGROW)
  ELSE
    HNEXT = 4.0 * H
  ENDIF
ENDIF
RETURN
END

```

```

*****
SUBROUTINE RKN4(X,Y,DYDX,H,YOUT,F)

```

```

*** Algorithm for fourth-order Runge-Kutta-Nystrom
*** integration of a second order system of differential
*** equations. On input, X, Y, and DYDX contain starting
*** values for the integration. H is the step size to be
*** tried. On output, X, DYDX, and YOUT contain the
*** values at the end of the step. F is a user-supplied
*** subroutine for calculating the value of the second
*** derivative.

```

```

IMPLICIT DOUBLE PRECISION (A-H,O-Z)
DOUBLE PRECISION DYDT(2), DYDX(2), K
COMMON /ERRORS/ ICALL, IERREPORT, IERROR
K = H / 2.0

```

```

A      = K * DYDX(2)
BETA   = K * (DYDX(1) + A/2.0)
DYDT(1) = DYDX(1) + A

```

```

CALL F(X+K, Y+BETA, DYDT)
IF (IERROR.GT.0) THEN
  RETURN
ENDIF

```

```

B      = K * DYDT(2)
DYDT(1) = DYDX(1) + B

```

```

CALL F(X+K, Y+BETA, DYDT)
IF (IERROR.GT.0) THEN
  RETURN
ENDIF

```

```

C      = K * DYDT(2)
DELTA = H * (DYDX(1) + C)
DYDT(1) = DYDX(1) + 2.0*C

```

```

CALL F(X+H, Y+DELTA, DYDT)
IF (IERROR.GT.0) THEN
  RETURN
ENDIF

```

```

D      = K * DYDT(2)
YOUT   = Y + H * ( DYDX(1) + (A+B+C)/3.0 )
DYDX(1) = DYDX(1) + ( A + 2.0*B + 2.0*C + D)/3.0
X      = X + H

```

```

CALL F(X, YOUT, DYDX)
IF (IERROR.GT.0) THEN
  RETURN
ENDIF

```

```

RETURN
END

```

```

SUBROUTINE PHYSICS_TEST(R, V, DVDR, ANS, KSTEP)

```

```

  DOUBLE PRECISION RTEST, RC, RB, R(7501), V(7501),
C DVDR(2,7501), DSLB, DSNB, DSLC, DSNC, VB, VC, RSAV,
C PI

```

```

  CHARACTER ANS

```

```

  DOUBLE PRECISION A, EO, LDEBYE, M_, MI, N_, NE,
C NI, NUM_ELEC, Q, T_, TE, VA
  DOUBLE PRECISION ALPHA, BETA1, BETA, LAMBDA
  DOUBLE PRECISION XOUT(7501), YOUT(7501),
C DYOUT(10,7501)

```

```

  PARAMETER (PI = 3.141592654)

```

```

  COMMON /ERRORS/ ICALL, IERREPORT, IERROR
  COMMON /PHYSICS/ A, EO, LDEBYE, M_, MI, N_, NE,
C NI, NUM_ELEC, Q, T_, TE, VA
  COMMON /PARAMETERS/ ALPHA, BETA1, BETA, IDIR,
C LAMBDA

```

```

COMMON /RESULTS/ XOUT, YOUT, DYOUT, KNEXT
COMMON /MISC/ RB,VB,RC,VC

DO J = 1, KNEXT

      V(J) = -EO * YOUT(J)
      R(J) = A / XOUT(J) * SQRT( SQRT( 4. / PI *
C 1836. * MI/BETA) * (ALPHA * EXP(VA / TE) + (1 -
C ALPHA) * SQRT( T_ / (TE * 1836. * M_) * EXP(VA /
C T_)))
      DVDR(1,J) = EO * XOUT(J)/R(J) * DYOUT(1,J)
      DVDR(2,J) = EO * (-2*XOUT(J)/R(J)**2 *
C DYOUT(1,J) - (XOUT(J)/R(J))**2 * DYOUT(2,J))
      R(J) = 1.0E4 * R(J)

      IF (ANS.EQ.'B'.OR.ANS.EQ.'S') THEN
        IF (MOD(J,KSTEP).EQ.0.OR.J.EQ.KNEXT) THEN
          WRITE (6,10) R(J),V(J),(DVDR(I,J),I=1,2)
        ENDIF
      ENDIF
      IF (ANS.EQ.'B'.OR.ANS.EQ.'F') THEN
        WRITE (44,10) R(J),V(J),(DVDR(I,J),I=1,2)
      ENDIF
10  FORMAT (4F15.3)
      ENDDO
      RETURN
      END

```

```

SUBROUTINE PHYSICS(R,V,DVDR)

      IMPLICIT DOUBLE PRECISION (A-H,L-Z)
      DOUBLE PRECISION R(7501),V(7501),DVDR(2,7501)
      DOUBLE PRECISION XOUT(7501), YOUT(7501),
C DYOUT(10,7501)

      PARAMETER (PI = 3.141592654)

      COMMON /ERRORS/ ICALL, IERREPORT, IERROR
      COMMON /PHYSICS/ A, EO, LDEBYE, M_, MI, N_, NE,
C NI, NUM_ELEC, Q, T_, TE, VA
      COMMON /PARAMETERS/ ALPHA, BETA1, BETA, IDIR,
C LAMBDA
      COMMON /RESULTS/ XOUT, YOUT, DYOUT, KNEXT
      COMMON /MISC/ RB,VB,RC,VC

      DSLB = 1000.

```


DSLCL = 100.

A = SQRT(ALPHA) * LDEBYE * BETA**0.75 /
 C SQRT(LAMBDA * SQRT(1836. * MI * 4. / PI) * (ALPHA *
 C EXP(VA / TE) + (1 - ALPHA) * SQRT(T_ / (TE * 1836.
 C * M_)) * EXP(VA / T_)))

YA = -VA/EO

DO J = 1, KNEXT

```
*          YOUT(J) = YOUT(J)*YA/YOUT(KNEXT)

          V(J) = -EO * YOUT(J)
          R(J) = A / XOUT(J) * SQRT( SQRT( 4. / PI *
C 1836. * MI / BETA) * (ALPHA * EXP(VA / TE) + (1 -
C ALPHA) * SQRT(T_ / (TE * 1836. * M_)) * EXP(VA /
C T_)))
          DVDR(1,J) = EO * XOUT(J)/R(J) * DYOUT(1,J)
          DVDR(2,J) = EO * (-2*XOUT(J)/R(J)**2 *
C DYOUT(1,J) - (XOUT(J)/R(J))**2 * DYOUT(2,J))
          RTEST
            = -3.0E4 * (DVDR(1,J)/DVDR(2,J))
          R(J)
            = 1.0E4 * R(J)

          DSNB = ABS(R(J)-RTEST)
          IF (DSNB.LE.DSLB) THEN
            DSLB = DSNB
            RB   = R(J)
            VB   = V(J)
            RSV  = RTEST
          ENDIF
          DSNC = ABS(ABS(V(J))-ABS(VA/10))
          IF (DSNC.LE.DSLC) THEN
            DSLC = DSNC
            RC   = R(J)
            VC   = V(J)
          ENDIF
        ENDDO

          Q          = -4.0 * PI * 8.854E-14 * A**2 *
C DVDR(1,KNEXT)
          NUM_ELEC = -Q/1.6021E-19

          RETURN
          END
```

```

SUBROUTINE ERROR_HANDLER(XO,XFINAL,TOL,SCALE)

IMPLICIT DOUBLE PRECISION (A-H,L-Z)

COMMON /ERRORS/ ICALL, IERREPORT, IERROR
COMMON /PARAMETERS/ ALPHA, BETA1, BETA, IDIR,
C LAMBDA

IF (IERREPORT.EQ.1) THEN
WRITE (36,*) 'WHILE INTEGRATING IN DIRECTION',
C IDIR
ENDIF

IF (IERROR.EQ.6) THEN
WRITE(36,*) 'ON CALL NUMBER', ICALL, ', Y <
C 0.0'
WRITE(6,*) 'ON CALL NUMBER', ICALL, ', Y <
C 0.0'

ELSE IF (IERROR.EQ.3) THEN
WRITE(36,*) 'ON CALL NUMBER', ICALL, ', X =
C 0.0'
WRITE(6,*) 'ON CALL NUMBER', ICALL, ', X =
C 0.0'
STOP

ELSE IF (IERROR.EQ.1) THEN
WRITE (36,*) 'ON CALL', ICALL
WRITE (36,*) 'SQUARE ROOT OF A NEGATIVE
C NUMBER'
STOP

ELSE IF (IERROR.EQ.2) THEN
WRITE (36,*) 'Y IS INCREASING AS X DECREASES'

ELSE IF (IERROR.EQ.4) THEN
WRITE (36,*) 'SUBROUTINE DRVTVS ATTEMPTED
C DIVIDE BY 0'
STOP

ELSE IF (IERROR.EQ.5) THEN
WRITE (36,*) 'RANGE OF X TOO LARGE'
WRITE (36,*) 'XO =', XO, ' XFINAL =', XFINAL
XFINAL = 7500 * SCALE * IDIR + XO
WRITE (36,*) 'NEW XFINAL =', XFINAL

ELSE IF (IERROR.EQ.10) THEN
WRITE (36,*) 'STEPSIZE INSIGNIFICANT IN RKQC'

```

```
WRITE (36,*) 'TOLERANCE IS TOO SMALL'
WRITE (36,*) 'OLD TOL = ', TOL
TOL = TOL * 1.1
WRITE (36,*) 'NEW TOL IS', TOL

ELSE IF (IERROR.EQ.11) THEN
WRITE (36,*) 'STEP SIZE SMALLER THAN MINIMUM IN
C ODEINT'
WRITE (36,*) 'TOLERANCE IS TOO SMALL'
WRITE (36,*) 'OLD TOL = ', TOL
TOL = TOL * 1.1
WRITE (36,*) 'NEW TOL IS', TOL

ELSE IF (IERROR.EQ.12) THEN
WRITE (36,*) 'TOO MANY STEPS IN ODEINT'
STOP

ELSE
WRITE (36,*) 'UNKNOWN ERROR, IERROR =', IERROR
WRITE (36,*) 'OCCURRED AT CALL ', ICALL
STOP
ENDIF

IERROR = 0

RETURN
END
```

REFERENCES

- [1] M. McCaughy and M. Kushner, "Electron Transport Coefficients in Dusty Argon Plasmas", *Applied Physics Letters*, vol. 55, no. 10, September 1989, pp. 951-953.
- [2] J. Trulsen and PTSG, "Plasma-Charged Particulate Interactions — Collisionless spherical probe theory revisited", University of California, Berkeley, July 1990.
- [3] G. Selwyn, J. Singh, and R. Bennett, "In-Situ Diagnostic Studies of Plasma-Generated Particulate Contamination", *J. Vac. Sci. Technol. A*, 7, Jul/Aug 1989, pp. 2758-2765.
- [4] G. Selwyn, J. McKillop, K. Haller, and J. Wu, "In-situ Plasma Contamination Measurements by HeNe Laser Light Scattering: A Case Study", to be published in *J. Vac. Sci. Technol.*
- [5] G. Selwyn, J. Heindenreich, and K. Haller, "Particle Trapping Phenomenon in Radio-Frequency Plasmas", IBM T.J. Watson Research Center, to be published.
- [6] J. Swift and M. Schwar, Electrical Probes for Plasma Diagnostics, Iliffe Books, Ltd., 1970, pp. 41-60.
- [7] I. Bernstein and I. Rabinowitz, "Theory of Electrostatic Probes in a Low-Density Plasma", *The Physics of Fluids*, vol. 2, no. 2, March-April, 1959, pp. 112-121.
- [8] E. Kreyszig, Advanced Engineering Mathematics, 5th ed., John Wiley & Sons, 1983, pp. 842-846.